

**The Efficacy and Specificity of Gold Nanoparticles as  
Antibiotics for *Klebsiella pneumoniae***

by

**Niki A. Osbaugh**

Department of Chemistry and Biochemistry

Defended April 3<sup>rd</sup>, 2015

Dr. Daniel Feldheim, Department of Chemistry and Biochemistry – Thesis Advisor

Dr. Joseph Falke, Department of Chemistry and Biochemistry – Honors Council Representative

Dr. Rolf Norgaard, Program for Writing and Rhetoric – Committee Member

Dr. Steve Schmidt, Department of Ecology and Evolutionary Biology – Committee Member

## Abstract

In 2013, the Centers for Disease Control and Prevention (CDC) declared antibiotic resistance a serious health threat to the global community. Multi-drug resistant (MDR) Gram-negative bacteria have become particularly problematic, as very few new classes of small-molecule antibiotics for Gram-negative bacteria have emerged in recent decades. The Feldheim Lab has developed a combinatorial screening process for identifying mixed-ligand monolayer gold nanoparticle conjugates with antibiotic activity. The gold nanoparticle conjugates have been found to be highly active against *E. coli*. The bacteria develop resistance to the nanoparticles at a significantly slower rate than commercially available small-molecule drugs.

The Feldheim Research Team has shown that the antimicrobial property of the nanoparticles depends on the identity and ratio of the ligands in the monolayer. Altering the ratio of one of the ligands from a conjugate designed for *E. coli* produced an altered conjugate with high levels of activity towards *K. pneumoniae*, and turned a bacteriostatic conjugate into a bactericidal conjugate. The altered conjugate also doubled the time to resistance over the initial nanoparticle formulation.

A differential gene expression experiment discovered that the altered conjugate affected a significantly increased number of genes compared to the original compound. It was determined that more active conjugates may alter the expression of many cell division proteins unchanged in the less active nanoparticles. In addition, the altered conjugate induced the expression of many antibiotic resistance genes, yet the bacteria remained susceptible to the conjugate for a number of days. The nanoparticle highly active toward *K. pneumoniae* was ineffective against *M. avium* and *M. abscessus*, possibly indicating bacterial specificity. The altered gold-nanoparticle conjugate was found to be an effective inhibitor of *K. pneumoniae* growth, with the possible ability to avoid resistance mechanisms.

## **Acknowledgements**

I would like to thank Dr. Daniel Feldheim for his continued support over the past three years. Working in the Feldheim Lab has been one of the most beneficial experiences of my undergraduate career. I would also like to thank Postdoctoral Fellow Dr. Carly J. Carter and PhD candidate Jennifer C. Gifford, who have been the most amazing mentors I could ever ask for. This honors thesis would not have been possible without their support, intelligence, and guidance. I would like to thank all of the past and present Feldheim Lab researchers who have helped me along the way.

The Undergraduate Research Opportunity Program (UROP), and the Howard Hughes Medical Institute (HHMI) Individual Grant, have allowed me to conduct my research over the past few years. Their financial support, along with their personal guidance, has opened up many doors for me. I would like to thank the UROP program for supporting students in the pursuit of research.

I cannot express my gratitude enough for John and Jan Lacher, and the Bob and Dickie Lacher Scholarship, who have believed in me, supported me, and allowed me to pursue many amazing opportunities these past three years. I would also like to recognize the Norlin Scholars Program for teaching me that success is defined in my own terms, and for encouraging me through every chapter of my undergraduate career.

I would not have been able to withstand the past four years without the amazing support and community of my fellow Biochemistry students, who never let a single Pi day, mole day, or e day pass by without celebration. Thank you to all of my friends who have become my nerdy family. Last but not least, I would like to thank my parents. Neither this honors thesis nor my graduation would be possible without their continued advice, love, and reassurance.

## **Table of Contents**

### **I. Introduction**

<b>Antibiotic Resistance and <i>Klebsiella pneumoniae</i></b> .....	<b>1</b>
<b>Interest in Gold Nanoparticles</b> .....	<b>4</b>
<b>Gold Nanoparticle Background Information</b> .....	<b>6</b>
Figure 1.1 .....	7
Table 1.1 .....	8
Figure 1.2 .....	8
Figure 1.3 .....	9
Table 1.2 .....	10
Figure 1.4 .....	12
Figure 1.5 .....	12
<b>Gold Nanoparticles as Antibiotics</b> .....	<b>14</b>

### **II. Methods**

<b>Synthesis of pMBA-Capped 2.0 nm Gold Nanoparticles</b> .....	<b>20</b>
<b>Place Exchange Reactions</b> .....	<b>21</b>
<b>Growth Inhibition Assay</b> .....	<b>22</b>
<b>Resistance Assay</b> .....	<b>23</b>
<b>Gene Expression Profiling</b> .....	<b>24</b>

### **III. Results and Discussion**

<b>Discovering Gold Nanoparticle Conjugates Active Toward <i>K. pneumoniae</i></b> .....	<b>27</b>
Table 2.1.....	28
<b>Altering the Active Conjugate to Increase <i>K. pneumoniae</i> Growth Inhibition</b> .....	<b>28</b>
Table 2.2.....	30
Table 2.3.....	31
Table 2.4 .....	32
<b>Determining the Time to Resistance for <i>K. pneumoniae</i></b> .....	<b>32</b>
Figure 2.1 .....	33
<b>Differential Gene Expression Experiment</b> .....	<b>35</b>
Figure 2.2 .....	36
<b>Analysis of Differentially Expressed Genes</b> .....	<b>37</b>

<b>A. Pathway Analysis of the Differentially Expressed Genes.....</b>	<b>38</b>
Table 2.5 .....	38
<b>I. Initial Metabolic Pathway Analysis Based on Ligand Structure.....</b>	<b>39</b>
Figure 2.3 .....	39
<b>II. Initial Metabolic Pathway Analysis Based on Cell Stress .....</b>	<b>40</b>
<b>B. Process Ontology to Further Analyze Metabolic Pathways.....</b>	<b>41</b>
Table 2.6 .....	41
Figure 2.4 .....	42
Figure 2.5 .....	43
<b>C. Individual DEG Analysis .....</b>	<b>44</b>
Table 2.7 .....	45
<b>I. DEGs Common to All Four Gold Nanoparticles.....</b>	<b>46</b>
<b>II. DEGs Common to All Three Active Conjugates .....</b>	<b>46</b>
<b>III. DEGs Unique to LAL-32 j .....</b>	<b>48</b>
Figure 2.6.....	49
Table 2.8 .....	50
<b>i. DEGs Unique to LAL-32 j Involved in Cell Division.....</b>	<b>51</b>
<b>ii. DEGs Unique to LAL-32 j Involved in Oxidative Stress.....</b>	<b>51</b>
<b>iii. DEGs Unique to LAL-32 j Involved in Antibiotic Resistance.....</b>	<b>52</b>
<b>LAL-32 j Tested Against M. avium and M. abscessus.....</b>	<b>54</b>
<b><u>IV. Conclusion</u></b>	

## **I. Introduction**

### **Antibiotic Resistance and *Klebsiella pneumoniae***

In 2013, the Centers for Disease Control and Prevention (CDC) declared antibiotic resistance a serious health threat to the global community.<sup>1</sup> In the U.S. alone, at least two million people are infected with antibiotic resistant bacteria every year and the contagions cause over 23,000 deaths annually.<sup>1</sup> In the 2013 Threat Report, CDC director Thomas Frieden examined the possibility of a post-antibiotic world, where minor cuts and injuries could be fatal due to the loss of antibiotic efficacy. Antibiotic resistance poses a large threat to modern society's vast medical advances. The loss of antibiotic efficacy would undermine the ability to perform surgeries, or conduct life saving treatments such as cancer chemotherapy and organ transplants. However, the emergence of drug resistant pathogens, and the battle against them, is not recent news. Examples of bacteria overcoming the effects of antibiotics have been reported since the introduction of antibiotics into society. Penicillin was discovered in 1929 by Sir Alexander Fleming, and released for clinical use in 1945.<sup>2</sup> Reports of penicillin resistance in some strains of *Staphylococci* came within one year of clinical release.<sup>3</sup> Within four years, 60 percent of British clinical isolates were penicillin resistant.<sup>3</sup> Today, about 70 percent of hospital-acquired infections are resistant to at least one form of antibiotic.<sup>4</sup>

Antibiotic resistance may be natural or acquired. Certain bacteria are inherently resistant to specific types of antibiotics. This natural resistance occurs in species that lack a target or transport system for the drug of interest. Antibiotic treatment can be made problematic if the bacteria have certain structural characteristics such as thicker cell walls or decreased expression of porins in the cell membrane.<sup>5</sup> Antibiotic resistance can also be acquired through spontaneous genetic mutation. Approximately one in one-billion bacteria undergo a mutation that allows for resistance, but considering high growth rates and high absolute numbers of cells obtained during

an infection, the time for an antibiotic resistant mutation to develop is relatively small.<sup>5</sup> Antibiotics put selective pressure on the bacterial colonies, thereby inhibiting the sensitive colonies, while also allowing resistant mutants to grow and divide. Resistant traits are passed on to their progeny through vertical evolution, as well as horizontal gene transfer.<sup>5</sup> Horizontal transfer of genetic information through plasmids allows resistant traits to be passed along within a single generation.

Four major mechanisms of resistance can occur in bacteria. The most common mode of resistance is enzymatic inactivation of antibiotics.<sup>5</sup> During enzymatic inactivation, cellular enzymes are modified to interact with an antibiotic in a way that renders the drug inactive. This process is exemplified by some bacteria's ability to alter Streptomycin, inhibiting the drug's ability to bind to the ribosome, thereby allowing transcription to proceed.<sup>5</sup> A second mode of resistance is the modification of the antibiotic target site, which removes the antimicrobial effect, and allows for proper bacterial growth.<sup>5</sup> Examples of the second mode of resistance can be observed in the penicillin binding proteins (PBPs), which are essential to cell wall biosynthesis and proliferation of the bacteria.<sup>6</sup> The PBPs catalyze the formation of peptidoglycan in the cell wall of bacteria.<sup>6</sup> Penicillin, a beta-lactam antibiotic, binds to the PBPs and inhibits peptidoglycan cross-linking.<sup>7</sup> The bacterium continues the dynamic process of cell wall renewal. Autolysis continues while cell wall formation is halted due to the antibiotic, ultimately weakening the cell wall. The destabilized cell envelope eventually bursts due to osmotic pressure. However, methicillin resistant *Staphylococcus aureus* produces a new penicillin binding protein, PBP2, which has low affinity for beta-lactam antibiotics.<sup>8</sup> PBP2 becomes the predominant PBP in the presence of beta-lactam antibiotics, and allows for cellular proliferation.<sup>8</sup> In the third resistant mechanism, enzymes may be produced that degrade

antibiotics.<sup>5</sup> This mode of resistance is seen in the carbapenemases. Carbapenems are beta-lactam antibiotics, similar to penicillin, with broad-spectrum activity toward both Gram-positive and Gram-negative bacteria.<sup>9</sup> The carbapenems permanently acylate the PBPs that catalyze the formation of peptidoglycan in the cell wall of bacteria, leading to cell lysis.<sup>9</sup> The most widespread mechanism of carbapenem resistance is the production of carbapenemases by the bacteria.<sup>9</sup> Carbapenemases are specific beta-lactamases, which are periplasmic enzymes, with the ability to hydrolyze the beta-lactam ring of carbapenems, altering the structure of the drug and rendering it ineffective.<sup>9</sup> Efflux pumps are the fourth mechanism of resistance, which allow for a wide range of resistance.<sup>10</sup> These high-affinity transport systems clear the antibiotic out of the bacterial cell, which is a major mode of resistance against tetracyclin antibiotics.<sup>10,5</sup> Together, these four key mechanisms of resistance have allowed bacteria to gain resistance to almost all commercially available antibiotics

The CDC has identified three different classes of bacteria that have significant levels of resistance and the ability to become widespread throughout the population at an extremely fast rate. High consequence antibiotic-resistant threats have been labeled as ‘Urgent Health Risks’ by the CDC.<sup>1</sup> These hazardous strains of bacteria include (1) *Clostridium difficile*, (2) cephalosporin-resistant *Neisseria gonorrhoeae*, and (3) Carbapenem-resistant *Enterobacteriaceae*.<sup>1</sup> The majority of the work described in this manuscript utilized *Klebsiella pneumoniae*, a member of the *Enterobacteriaceae* class. *K. pneumoniae* is a Gram-negative, encapsulated, rod-shaped facultative anaerobe.<sup>11</sup> This bacterium causes pneumonia, bloodstream infections, surgical site infections, and meningitis.<sup>12</sup> Some reported strains of *Klebsiella* have become resistant to every antibiotic commercially available.<sup>1</sup> The carbapenem-resistant strains are of particular concern

due to the fact that carbapenems are generally last resort antibiotics.<sup>1</sup> The carbapenem-resistant *Klebsiella* is responsible for 7,900 drug-resistant infections every year.<sup>1</sup>

The fast rates of antibiotic resistance and multi-drug resistance have made the development of new antibiotics difficult. Between 1960 and 2000, there were only three new classes of antibiotics introduced in the medical community.<sup>13</sup> This is problematic because bacteria are quickly gaining resistance to the available classes of antibiotics. Doctors and researchers alike have been working toward developing new antibiotic materials to overcome the increase in antibiotic resistance. In 2014, the discovery of oxadiazoles introduced a new class of antibiotics that inhibit the penicillin-binding protein PBP2a, thereby inhibiting penicillin-resistant forms of bacteria.<sup>14</sup> However, it is only a matter of time before the bacteria evolve beyond this type of antibiotic. It is evident that new classes of antibiotics, which avoid the various mechanisms of resistance, must be developed in order to combat the rise in antibiotic resistance.

### **Interest in Gold Nanoparticles**

The search to find new classes of antibiotics has led researchers to look outside the classical, small molecule antibiotics, toward organic and inorganic nano-materials.<sup>15,16,17</sup> A vast number of nanoparticles have been synthesized, predominately those made from noble metals such as gold. There is a large interest in utilizing gold nanoparticles because they provide non-toxic transporters for drug and gene delivery applications.<sup>17</sup> Gold nanoparticles are clusters of gold surrounded by a monolayer of selected ligands.<sup>17</sup> The gold core is essentially inert, non-toxic, and imparts stability to the assembly of molecules. The monolayer of ligands allows for tunable properties such as charge and hydrophobicity.<sup>17</sup> An additional attractive property of the gold nanoparticles are their interactions with thiols. The attachment of ligands through sulfur

bonds has allowed the Feldheim Lab to select and attach molecules with a variety of properties to construct custom antibiotics.

This experiment utilizes the thiol-protected gold nanoparticles as antibiotics with a variety of thiol-ligands. Gold was chosen for the nanoparticle core due to its ability to create a wide variety of sizes, ranging from 1 nm to 150nm.<sup>17</sup> The Feldheim Lab has focused on nanoparticles with a diameter of 1 – 5 nm. The average core size can be adjusted by changing the preparative conditions, such as the gold:ligand ratio, the reaction temperature, and the reducing agent.<sup>18</sup> Gold consistently produces monodispersed nanoparticles and has an easily exchanged surface monolayer, which allows for a wide diversity of nanoparticle conjugates. Mass spectrometry and x-ray crystallography data are available for various nanoparticles, including those with base aggregates of 25, 38, 102, and 144 molecules of gold.<sup>19,20,18,21</sup> Au-25 and Au-38 are about 1 nm in diameter, while Au-102 and Au-144 are 1.5 nm and 2.0 nm respectively. These gold nanoparticles were found to have true chemical formulas such as  $[\text{Au}_{144}(\text{SC}_6\text{H}_4\text{COOH})_{60}]$  for Au-144.<sup>21</sup>

During gold nanoparticle synthesis,  $\text{AuCl}_4^-$  salts are reduced with  $\text{NaBH}_4$  in the presence of a thiol capping ligand.<sup>19</sup> Initial gold nanoparticles are capped with passivating ligands, which can subsequently be exchanged for other types of molecules. In this associative type place exchange reaction, incoming thiol ligands displace existing ligands, creating a mixed thiol monolayer surrounding the gold nanoparticle.<sup>22</sup> The gold nanoparticles are stabilized by this organothiol shell.<sup>18</sup> The thiol modification allows for the construction of libraries with large numbers of distinct gold-nanoparticle conjugates that can be screened for antibiotic activity.

Gold nanoparticles have many attributes that distinguish them from the traditional, small molecule antibiotics. These characteristics make them good drug candidates to combat multi-

drug resistant pathogens. Nanoparticles can be constructed in a range of sizes, allowing for variance and adaptation of the antibiotic. The methods for synthesizing the gold nanoparticles are easily reproducible and yield water-soluble compounds. This allows for simple production, storage, and delivery of the antimicrobial agent. In nanoparticle synthesis, two or more ligands can be attached to a single particle to create multivalent and multifunctional systems.<sup>23</sup> Small molecule drugs often have short blood circulation half-lives, but conjugation to a nanoparticle can prolong the *in vivo* circulation time from several minutes to several hours.<sup>24</sup> The increased blood circulation half-life of the gold nanoparticle conjugates would provide less frequent administration of the drug and more effective antimicrobial therapy. Small-molecule drugs often rely upon a single high-affinity contact to a microbial target, and are typically incapable of disrupting protein-protein interactions.<sup>23</sup> Small-molecule drugs are also easily expelled from the microbial cell through efflux pumps.<sup>5</sup> The diameter of the nanoparticles are slightly larger than drug efflux pumps, indicating the possibility of avoiding antibiotic resistance more effectively than traditional, small-molecule antibiotics.<sup>24</sup> The size of the gold nanoparticles could also provide them with the ability to disrupt protein-protein interactions.<sup>25,26,27,28</sup> These characteristics give the gold nanoparticles many possible advantages over small-molecule drugs.

### **Gold Nanoparticle Background Information**

The Feldheim Lab aspires to utilize gold nanoparticles as antibiotics to combat multi-drug resistant pathogens. In order to screen the nanoparticles for antibiotic activity, an initial library of conjugates was created using a Small-Molecule Variable Ligand Display (SMVLD) method. This library is a catalog of all the gold nanoparticle conjugates created, as well as their efficacy as an antibiotic agent against the bacteria of interest. The mixed monolayer gold nanoparticle combinatorial library was created on ~2.0 nm diameter gold nanoparticles coated

with para-mercaptobenzoic acid (pMBA).<sup>23</sup> Place-exchange reactions subsequently substitute some of the para-mercaptobenzoic acid in the monolayer with varying thiols of choice. Figure 1.1 illustrates a simplified model of the gold nanoparticles before and after the place exchange reactions with three thiol-ligands.

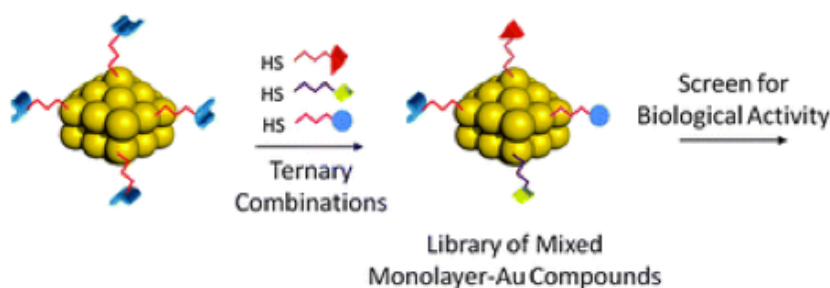


**Figure 1.1 Thiol-Ligands in Ternary Combination Replace pMBA Molecules in the Monolayer of the Gold Nanoparticle** (Figure from Bresee, J.; Maier, K. E.; Melander, C.; Feldheim, D. L. *Chem. Commun.* 2010, 46, 7516–7518.)

The initial library utilized ten commercially available thiols, combined in groups of three, with varying feed ratios. The feed ratio is the stoichiometric molar ratio of ligand input to gold nanoparticle input. The combination and ratio of the different thiol ligands has been shown to be vital to the antimicrobial efficacy of the gold nanoparticles.<sup>29</sup> The thiol-ligands have a range of attributes with varying Hydrogen-bond donors and acceptors, as well as hydrophilic/hydrophobic properties that may contribute to the antimicrobial nature of the gold nanoparticles. The chemical characteristics of the thiols can be found in Table 1.1, with the structures found in Figure 1.2.

Table 1.1 Thiol Name and Chemical Characteristics

Thiol Number	Thiol Name	Characteristic
1	3-Nitrobenzyl mercaptan	Hydrophobic
2	3-methyl - 1 - butanethiol	Hydrophobic
3	4-mercaptophenol	Antimicrobial, Amino Acid Structure
4	4-aminothiophenol	Hydrophobic
5	Glutathione	Water Soluble, Amino Acid Structure
6	Cysteamine	Amino Acid Structure, Hydrophobic
7	Thioglucose	Sugar Structure
8	3-mercapto-1-propanesulfonic acid	Water Soluble
9	2 - diethylaminoethane thiol	Hydrophobic
10	N-(methyl) mercaptoacetamide	Hydrophobic

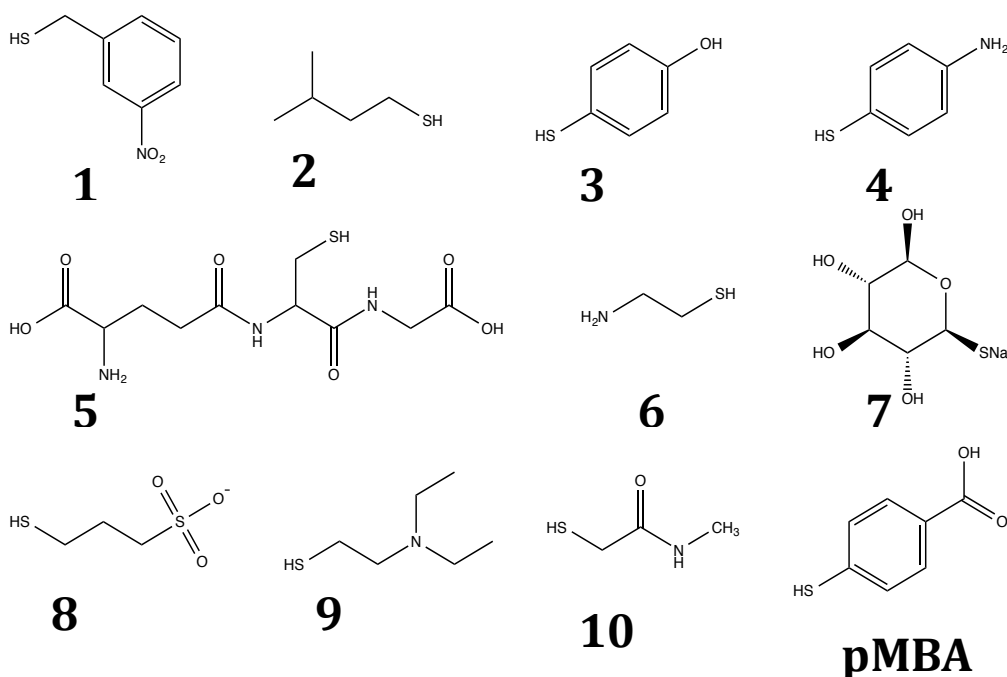


Figure 1.2 Structure of Thiol Ligands

The number of diverse compounds produced in a library can be calculated using the formula:

$$\text{number of compounds} = (m!)/[n!(m - n)!]$$

where  $m$  = number of thiols in the library and  $n$  = number of thiols in the exchange reaction.

The initial library of ten thiols, combined in groups of three, produced 120 distinct nanoparticle conjugates, many of which had antimicrobial properties.<sup>23</sup>

After the initial library construction, additional ligands such as thiol 11 were added for expanded diversity. Antimicrobial cationic peptides are well documented as part of the innate immune system of eukaryotes as a defense against pathogens.<sup>30</sup> The positive charge on molecules such as arginine, lysine, and histidine have been found to interact with the negatively charged bacterial membrane. Thiol 11 is 3-(1H-imidazol-4-yl)-2-(((5-mercapto-3-oxopentyl)oxy)amino)propanoic acid, and is similar in structure to the amino acid histidine with a short polyethylene glycol linker. The structure of ligand 11 can be seen in Figure 1.3.

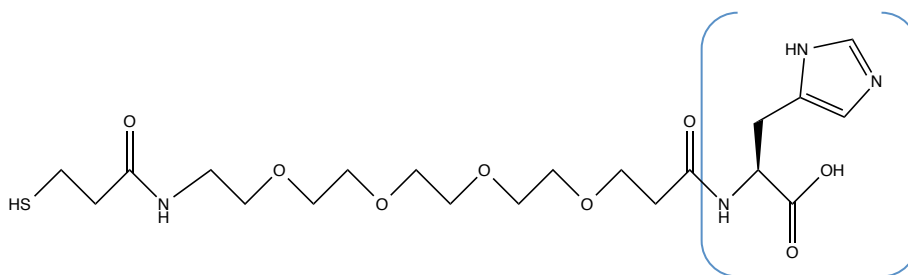


**Figure 1.3: Structure of Thiol 11 - A Thiolated Histidine Molecule (Histidine Structure in Brackets)**

Several different nanoparticle conjugates in the library were found to be potent growth inhibitors of *Escherichia coli* (ATCC 25922).<sup>29</sup> Table 1.2 highlights gold nanoparticles of interest that inhibit *E. coli*, the combination of thiol ligands, and the concentration of nanoparticles required to inhibit 99.9% of bacterial growth (MIC<sub>99.9</sub>), determined by plating and colony count.<sup>29</sup> The nanoparticles reported in Table 1.2, particularly LAL-32, have high bacterial inhibition rates and have formed the foundation of this honors thesis.

**Table 1.2 List of Gold Nanoparticle Conjugates and MIC<sub>99.9</sub> Values for the Inhibition of *E. coli* (ATCC 25922).** (Figure from Bresee, J.; Melander, C.; Feldheim, D. L. *J. Am. Chem. Soc.* 2014, 136, 5295–5300.)

Conjugate ID	Thiol A	Thiol B	Thiol C	MIC <sub>99.9</sub> (μM)
LAL-32	5	6	8	0.25
LAL-33	6	8	9	0.5
LAL-42	6	8	-	0.5
LAL-52	5	6	11	0.25

The LAL gold nanoparticle conjugates contain a monolayer of designated thiol ligands mixed with pMBA. The pMBA-capped nanoparticles with no additional thiol ligands were found to have no significant inhibitory activity at concentrations tested up to 50 μM. These tests confirm the thiol ligands provide antibiotic activity to the gold nanoparticles.<sup>29</sup> The experiments also showed that the ligands must be bound to the surface of the nanoparticle to be active.<sup>29</sup> The conjugate LAL-32 was experimentally determined to be approximately 360x more active per ligand than its corresponding free ligands (5, 6 and 8).<sup>29</sup> This free-ligand experiment demonstrated that the gold nanoparticle conjugated to the mixed-ligand monolayer acts as a single entity antibiotic. The gold nanoparticle antibiotics contrast nanoparticle delivery systems previously utilized in the field. Solid-state Nuclear Magnetic Resonance (NMR) spectroscopy confirmed the conjugation of pMBA and the thiol ligands to the active gold-nanoparticle, thus verifying the presence of a mixed monolayer.<sup>23</sup>

Detailed characterization of the nanoparticles was important to determine how the nanoparticles may be interacting with the bacteria. For example, LAL-32, found to be one of the most potent inhibitors of *E. coli* growth, contains a core diameter of 2.4 nm ± 0.6 nm.<sup>29</sup> This is a slight increase over the pMBA-capped gold nanoparticle starting material, which had a diameter of 2.2 nm ± 0.4 nm.<sup>29</sup> The diameter of the nanoparticle is particularly important in bacterial studies as it determines the scale on which the drug can interact with the bacteria, as well as if

the bacteria can easily excrete the molecule. It was estimated that on average, the monolayer of LAL-32 contains 11 p-mercaptobenzoic acids, 33 glutathiones (5), 28 cysteamines (6), and 15 3-mercapto-1-propanesulfonic acids (8).<sup>29</sup>

Several experiments were performed to help elucidate the mode of action of the nanoparticles. A BacLight Permeability assay performed with LAL-32 showed that membrane disruption did not occur in the *E. coli* strain tested.<sup>29</sup> Experiments revealed that the nanoparticle conjugates are generally not cytotoxic, nonspecific cell membrane disruptors, but rather affect the transcription of several genes.<sup>29</sup> This data is important because it confirmed the nanoparticles are not “nuisance compounds.” Nuisance compounds are molecules that act equally on bacterial and mammalian cells, and are detrimental to all cell types. The gold nanoparticles selectively inhibit bacterial cell growth, which allows for possible use as an antibiotic *in vivo*. Transmission Electron Microscopy experiments with *E. coli* showed internalization of nanoparticles into the cell, indicating the ability to reach intercellular targets.<sup>29</sup> Figures 1.4 and 1.5 show *E. coli* cells incubated with conjugate LAL-32 for one hour and six hours respectively, effectively demonstrating the nanoparticle conjugates internalization into the cell.

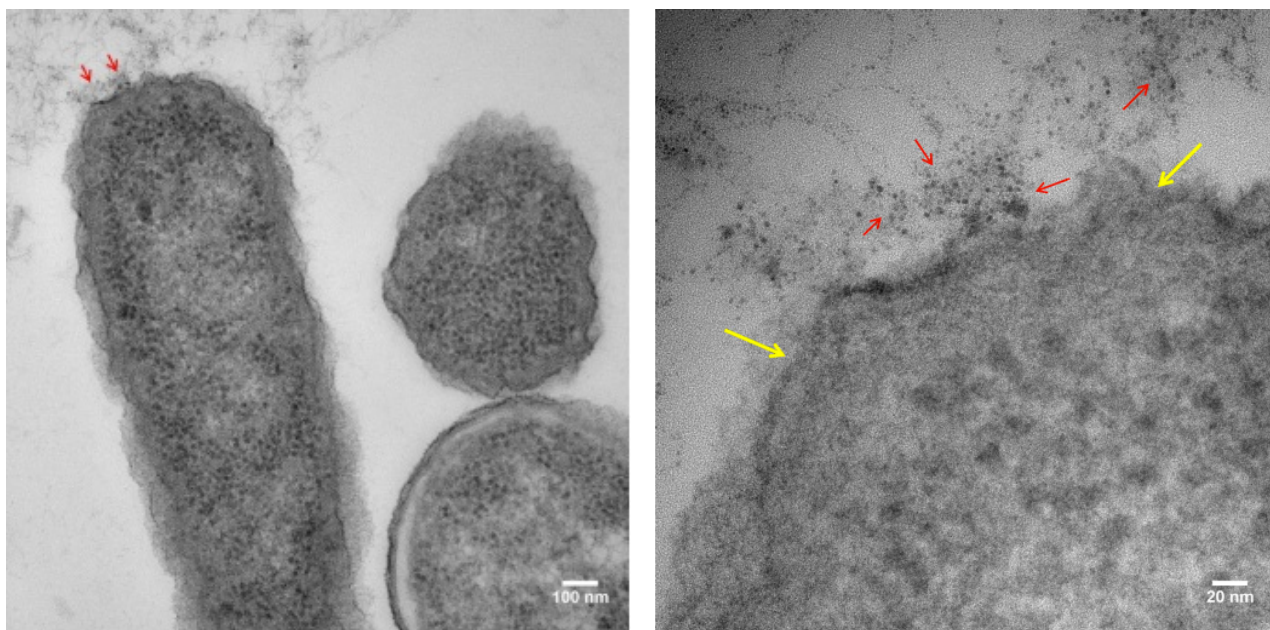


**Figure 1.4:** Transmission electron microscope images of sectioned ( $\sim 60$  nm) *E. coli* incubated with LAL-32 for 1 hr. The red arrows indicate nanoparticles; the yellow arrows indicate bacteria membrane. (Figure from Bresee, J.; Melander, C.; Feldheim, D. L. *J. Am. Chem. Soc.* 2014, 136, 5295–5300.)

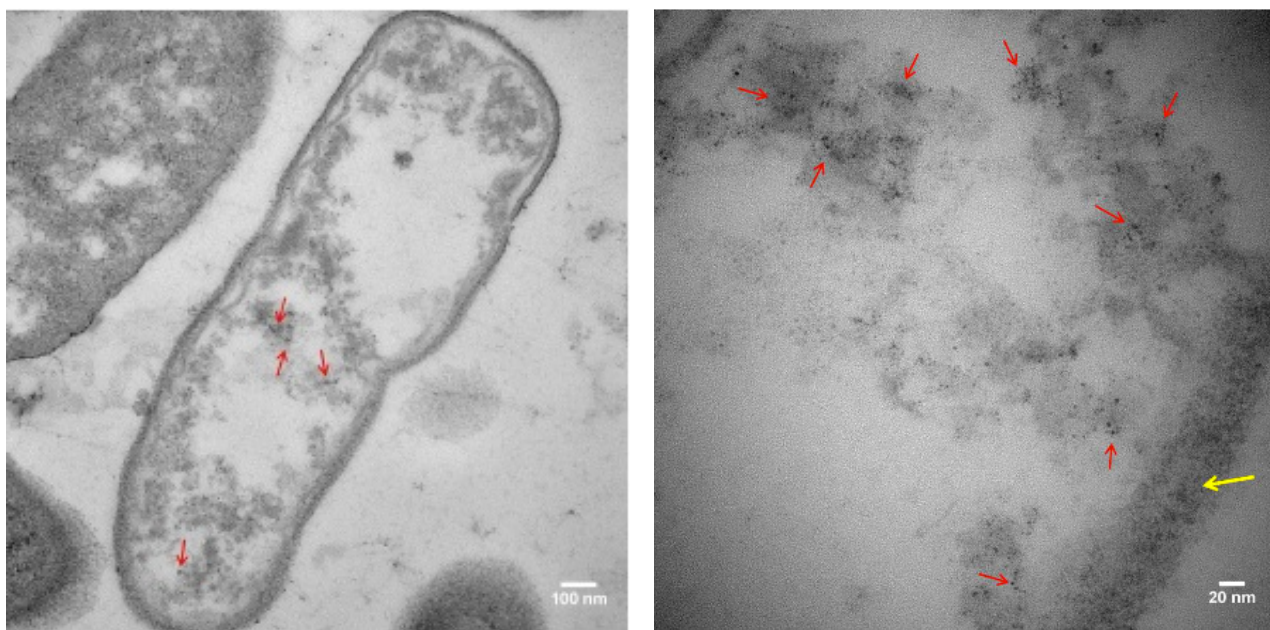


**Figure 1.5:** Transmission electron microscope images of sectioned ( $\sim 60$  nm) *E. coli* cells incubated with LAL-32 for 6 hr. The red arrows indicate nanoparticles; the yellow arrows indicate bacterial membrane. (Figure from Bresee, J.; Melander, C.; Feldheim, D. L. *J. Am. Chem. Soc.* 2014, 136, 5295–5300.)

The gold nanoparticles' ability to reach intracellular targets led to gene expression experiments to further elucidate the mode of action. The genetic pathways most altered may indicate how the gold nanoparticles were affecting the bacteria. *E. coli* samples were incubated with pMBA only nanoparticles (control sample), as well as active LAL-32 conjugates. The RNA was then extracted and analyzed to determine which genes had been upregulated/downregulated when exposed to either treatment. Microarray experiments found 154 genes that were differentially expressed in *E. coli* upon exposure to LAL-32 compared to untreated cells.<sup>29</sup> Evidence showed an up-regulation of genes encoding for metabolic pathway components, efflux pumps, membrane proteins, and multiple antibiotic resistance genes (*mar*) upon exposure to active gold nanoparticle conjugates.<sup>29</sup> The *mar* gene products confer resistance to many structurally unrelated small-molecule drugs, including chloramphenicol, fluoroquinolones, and tetracycline.<sup>31</sup> The *mar*-associated resistance occurs through increased production of efflux pumps to excrete the small-molecule drugs.<sup>31</sup> The up-regulation of *mar* genes in the bacteria did not diminish the inhibitory effects of LAL-32. This indicated that the intrinsic cellular machinery in *E. coli* to confer antibiotic resistance was not adequate to counteract the effects of the nanoparticle.

The gene expression experiment also determined that gold nanoparticle exposure caused a down-regulation in many transcriptional regulators and cell division proteins.<sup>29</sup> DicC specifically was down-regulated upon exposure to LAL-32 compared to the pMBA-capped gold nanoparticle.<sup>29</sup> DicC is involved in the control of cell division, including activation of the Min family of proteins, which regulate the location of FtsZ polymerization.<sup>32,33</sup> Most bacterial cell division is initiated by the formation of the Z-ring, which consists of a dynamic structure of FtsZ polymers.<sup>34</sup> The Z-ring's location is determined by negative regulators of FtsZ assembly, which

recruits additional division proteins to form the septal ring, separating the two progeny cells.<sup>35</sup> The septum occurs in the area where the concentration of these negative regulators is at a minimum. Experiments showed that the gold nanoparticle conjugate LAL-32 down-regulates some of these negative regulators and therefore may affect proper formation of the Z-ring during cell division.<sup>29</sup>

### **Gold Nanoparticles As Antibiotics**

The Feldheim Research Group has demonstrated that nanoparticle activity depends on the specific combination of ligands attached to the particle surface. Some of the most potent nanoparticle conjugates inhibit 99.9% of *E. coli* growth at a minimum inhibitory concentration (MIC<sub>99.9</sub>) of 250 nM.<sup>29</sup> LAL-32 and LAL-52 are therefore more potent antibiotics than many small-molecule antibiotics on the market currently, such as ampicillin (MIC of 11  $\mu$ M), gentamicin (MIC of 1  $\mu$ M), and chloramphenicol (MIC 12  $\mu$ M).<sup>36,37</sup>

The emergence of multi-drug resistant pathogens has made developing antibiotics that avoid or increase the time to resistance of great importance. Experiments have shown that *E. coli* developed resistance against the nanoparticles significantly slower than chloramphenicol, a commercially available small-molecule drug.<sup>29</sup> Even after 50 days of exposure, *E. coli* was not able to gain significant resistance to the gold nanoparticle conjugate LAL-32.<sup>29</sup> In contrast, *E. coli* was able to develop resistance to chloramphenicol within two days of exposure.<sup>29</sup> The time to resistance had significant variance between conjugates, and was dependent on the identity and ratio of the thiol ligands in the mixed monolayer. The nanoparticles have the potential to greatly reduce the speed at which pathogens gain resistance to antibiotics. This feature increases the potential to treat multi-drug resistant pathogens with gold nanoparticles, combatting the global issue of antibiotic resistance.

The Feldheim Lab has performed numerous experiments to determine the potential use of gold nanoparticles as drugs *in vivo*. Blood hemolysis assays performed on defibrinated sheep blood cells found that within experimental error, no hemolysis was observed for LAL-33, LAL-42, or LAL-52 even at 100x the MIC<sub>99,9</sub>.<sup>29</sup> This indicates that there was high selectivity of the active nanoparticle conjugates for bacterial cell growth inhibition over mammalian cell hemolysis. MTT toxicity assays also established that the gold nanoparticle conjugates were not toxic to human liver cells (HepG2/2.2.1, ATCC CRL -11997) in concentrations up to 0.8 μM.<sup>29</sup> The Feldheim Research Team demonstrated that the *in vivo* biodistribution, clearance, and toxicity of ligand-modified gold nanoparticles depend on the ligands in the monolayer, which enables them to be easily adjusted. Glutathione-modified gold nanoparticles are primarily cleared through the renal system, and do not cause any toxicity or morbidity.<sup>38,39</sup> Although the LAL-32 conjugate behaved similarly to the glutathione-modified nanoparticles at low concentrations (10 μM), it caused renal complications at higher concentrations (60 μM).<sup>29</sup> By adding a thiolated oligoethyleneglycol into the mixed monolayer of LAL-32, the nanoparticle LAL-32EG was produced, which showed no *in vivo* toxicity at high concentrations, and maintained an identical bacterial growth inhibition efficacy.<sup>29</sup>

The Feldheim Lab injected mice with 200 μL of 60 μM LAL-32EG, and found the nanoparticles were cleared primarily through the kidneys, and blood circulation half-life was estimated to be 7 hours ± 3 hours.<sup>29</sup> Furthermore, the addition of polyethylene glycol (PEG) into the monolayer of the nanoparticle dramatically enhanced the absorption of the gold nanoparticles in the gastrointestinal tract.<sup>29</sup> This information demonstrated that the mixed thiol monolayer gold nanoparticles are possible candidates for novel orally bioavailable antibiotics.

The Feldheim Lab utilized *E. coli* to demonstrate the gold nanoparticles' potential as an antibiotic. The same Small Molecule Variable Ligand Display (SMVLD) method of developing gold nanoparticles that inhibit the growth of *E. coli*, can also be utilized to find potent inhibitors of other bacteria of interest, such as *Klebsiella pneumoniae*. It is particularly important to find antibiotics that are active against *Klebsiella pneumoniae* and also avoid resistance mechanisms. Early in 2015, two deaths, seven confirmed infections, and 179 possible exposures to Carbapenem-Resistant *Enterobacteriaceae* (CRE) were reported in a Los Angeles hospital.<sup>40</sup> The CRE are resistant to all, or nearly all, available antibiotics, including the most powerful drugs of last-resort.<sup>41</sup> The CDC has warned that the CRE are spreading in hospital settings, and have reported a 50% death rate among patients who acquire a CRE bloodstream infection.<sup>41</sup> This honors project aimed toward finding a highly potent gold nanoparticle conjugate that is effective against *Klebsiella pneumoniae*, while overcoming potential antibiotic resistance.

## Bibliography

- [1] Frieden, T. Antibiotic Resistance Threats in the United States, **2013**.
- [2] <http://www.hardydiagnostics.com/articles/Fleming-and-Penicillin.pdf>.
- [3] Stearns, S. C.; Koella, J. C. *Evolution in Health and Disease*; Oxford University Press, **2007**.
- [4] Battle of the Bugs: Fighting Antibiotic Resistance. *U.S. Food and Drug Administration*, **2011**.
- [5] Todar, K. *Todar's Online Textbook of Bacteriology*. **2011**.
- [6] Macheboeuf, P.; Contreras-Martel, C.; Job, V.; Dideberg, O.; Dessen, A. *FEMS Microbiol. Rev.* **2006**, *30* (5), 673–691.
- [7] Yocum, R.; Rasmussen, J.; Strominger, J. *The Journal of Biological Chemistry*. **1980**, Vol. *225*, *9*, 3977-3986.
- [8] Katayama, Y.; Zhang, H.; Chambers, H.F. *Antimicrobial Agents and Chemotherapy*. **2004**, *48*, 453-459.
- [9] Papp-Wallace, K. M.; Endimiani, A.; Taracila, M. A.; Bonomo, R. A. *Antimicrob Agents Chemother* **2011**, *55*.
- [10] Borges-Walmsley, M.I.; McKeegan, K.S.; Walmsley, A. R. *Biochem J.* **2003**, *376*, 313-338.
- [11] Brisse, S.; Francine, G.; Grimont, P. "The genus *Klebsiella*." *The Prokaryotes*. Springer New York, **2006**, 159-196.
- [12] *Klebsiella pneumoniae* in Healthcare Settings, *Centers for Disease Control*. **2012**.
- [13] The Royal Society of Chemistry, *The Trouble with Antibiotics*, **2003**.  
<http://www.rsc.org/chemistryworld/Issues/2008/March/TheTroubleWithAntibiotics.asp>.
- [14] O'Daniel, P. I.; Peng, Z.; Pi, H.; Testero, S. A.; Ding, D.; Spink, E.; Leemans, E.; Boudreau, M. A.; Yamaguchi, T.; Schroeder, V. A.; Wolter, S.; Chang, M. *J. Am. Chem. Soc.* **2014**, *136*, 3664–3672.
- [15.] Page-Clisson, M.E.; Pinto-Alphandary, H.; Ourevitch, M.; Andreumont, A.; Couvreur, P. *Journal of Controlled Release*. **1998**, *56*, 23-32.
- [16] Turos, E.; Shim, J.; Wang, Y.; Greenhalgh, K.; Reddy, G.S.K.; Dicky, S.; Lim, D.V. *Bioorg. Med. Chem. Lett.* **2007**, *17*, 53-56.

- [17] Ghosh, P.; Han, G.; De, M.; Kim, C. K.; Rotello, V. M. *Advanced Drug Delivery Reviews*. **2008**, *60*, 1307–1315.
- [18.] Jadzinsky, P.D.; Calero, G.; Ackerson, C.J.; Bushnell, D.A.; Kornberg, R.D. *Science*. **2007**, *318*, 430-433.
- [19] Shichibu, Y.; Negishi, Y.; Tsunoyama, H.; Kanehara, M.; Teranishi, T.; Tsukuda, T. *Small*. **2007**, *3*, 835-839.
- [20] Qian, H.; Eckenhoff, W. T.; Zhu, Y.; Pintauer, T.; Jin, R. *J. Am. Chem. Soc.* **2010**, *132*, 8280-8281.
- [21] Lopez-Acevedo, O.; Akola, J.; Whetten, R.L.; Grönbeck, H.; Häkkinen, H. *J. Phys. Chem. C*, **2009**, *113*, 5035-5038.
- [22] Templeton, A.C.; Wuelfing, W.P.; Murray, R.W. *Acc. Chem. Res.* **2000**, *33*, 27-36.
- [23] Bresee, J.; Maier, K. E.; Melander, C.; Feldheim, D. L. *Chem. Commun.* **2010**, *46*, 7516–7518.
- [24] Zhang, L.; Gu, F. X.; Chan, J. M.; Wang, A. Z.; Langer, R. S.; Farokhzad, O. C. **2007**. Nanoparticles in medicine: therapeutic applications and developments. *Clinical Pharmacology & Therapeutics*, *83*(5), 761-769.
- [25] H. Bayraktar, P. S. Ghosh , V. M. Rotello , M. J. Knapp , *Chem. Commun.* 2006. 1390 – 1392. \*This citation has the initials presented in the opposite fashion from the rest.
- [26] Fischer, N. O.; McIntosh, C. M.; Simard, J. M.; Rotello, V. M. *Proc. Natl. Acad. Sci. U.S.A.* **2002**, *99*, 5018–5023.
- [27] De, M.; You, C. C.; Srivastava, S.; Rotello, V. M. *J. Am. Chem. Soc.* **2007**, *129*, 10747–10753.
- [28] Boal, A. K.; Rotello, V. M. *J. Am. Chem. Soc.* **2000**, *122*, 734–735.
- [29] Bresee, J.; Bond, C. M.; Worthington, R. J.; Smith, C. A.; Gifford, J. C.; Simpson, C. A.; Carter, C. J.; Wang, G.; Hartman, J.; Osbaugh, N. A.; Shoemaker, R. K.; Melander, C.; Feldheim, D. L. *J. Am. Chem. Soc.* **2014**, *136*, 5295–5300.
- [30] Hancock, R. E.; Diamond, G. *Trends Microbiol.* **2000**, *8*, 402–410.
- [31] Poole, K. *J. Antimicrob. Chemother.* **2005**, *56* (1), 20–51.
- [32] Béjar, S.; Bouché, F.; Bouché, J. P. *Mol. Gen. Genet.* **1988**, *212* (1), 11–19.

- [33] Bi, E.; Lutkenhaus, J. *J. Bacteriol.* **1993**, *175* (4), 1118–1125.
- [34] Symposium, S. for G. M. *Prokaryotic Structure and Function: A New Perspective : Forty-seventh Symposium of the Society for General Microbiology Held at the University of Edinburgh, April 1991*; Cambridge University Press, **1992**.
- [35] Lutkenhaus, J. In *Encyclopedia of Life Sciences*; John Wiley & Sons, Ltd, Ed.; John Wiley & Sons, Ltd: Chichester, UK, **2009**.
- [36] J. M. Andrews, *J. Antimicrob. Chemother.* **2001**, *48*(1), 5.
- [37] D. Corogeanu, R. Willmes, M. Wolke, G. Plum, O. Utermöhlen and M. Krönke, *BMC Microbiol.* **2012**, *12*, 160.
- [38] Smith, C.; Kim, C. A. S.; Carter, C. J.; Feldheim, D. L. *ACS Nano* **2013**, *7*, 3991.
- [39] Simpson, C. A.; Salleng, K. J.; Clifffel, D. E.; Feldheim, D. L. *Nanomedicine* **2013**, *9*, 257–263.
- [40] Drug-resistant bacteria linked to two deaths at UCLA hospital - CNN.com  
<http://www.cnn.com/2015/02/18/health/california-deadly-bacteria/index.html> (accessed Feb 21, 2015).
- [41] CDC Online Newsroom - New CDC Vital Signs: Lethal, Drug-resistant Bacteria Spreading in U.S. Healthcare Facilities <http://www.cdc.gov/media/dpk/2013/dpk-vs-hai.html> (accessed Feb 21, 2015).

## II. Methods

### Synthesis of pMBA- Capped 2.0 nm Gold Nanoparticles

The two nanometer diameter  $[\text{Au}_{144}(\text{SC}_6\text{H}_4\text{COOH})_{60}]$  gold nanoparticles were synthesized in a three-day process, previously described by the Feldheim Lab.<sup>1</sup> Approximately 136 mg of  $\text{HAuCl}_4 \cdot 3\text{H}_2\text{O}$  (Sigma-Aldrich) was dissolved in 20 mL of methanol at room temperature with constant stirring in a 50 mL Erlenmeyer flask. Simultaneously, 210 mg of para-mercaptobenzoic acid (pMBA) (TCI-America) was then dissolved in 15.4 mL of ultrapure  $\text{H}_2\text{O}$  and 0.6 mL of 10 M NaOH. The pMBA solution was then added to the gold/methanol solution and covered with parafilm. The solution was allowed to react overnight with constant stirring.

After 16 to 18 hours, the solution was divided equally between three 500 mL Erlenmeyer flasks, followed by the addition of 62 mL of methanol and 178 mL of ultrapure  $\text{H}_2\text{O}$  to each flask. A 0.25 M solution of sodium borohydride (Sigma Aldrich) was freshly prepared and 2.4 mL were immediately added to each flask. Adding 24 mL of ultrapure  $\text{H}_2\text{O}$  further diluted each solution. The nanoparticle formation reaction was allowed to react for 24 hours with constant stirring.

After 24 hours, the gold nanoparticles were harvested. The addition of 2 mL of 5.0 M NaCl and 150 mL of methanol to each flask caused nanoparticle precipitation. The nanoparticles were then pelleted by centrifugation at 3200x g for 5 minutes in 50 mL conical tubes. The pellets were dried overnight, and subsequently re-suspended in filter-sterilized ultrapure  $\text{H}_2\text{O}$ . The gold nanoparticles were then washed on 10k M.W.C.O. filters (Millipore) with filter-sterilized ultrapure  $\text{H}_2\text{O}$  and centrifuged five times for 6 minutes at 3200x g, followed by a sixth round for 8 minutes at 3200x g. Nanoparticle

concentration was determined through UV-visible spectroscopy using the  $\epsilon_{510\text{nm}}$  of  $409,440 \text{ M}^{-1}\text{cm}^{-1}$ .

The source and age of the reagents in gold nanoparticle synthesis are important in preparation, as well as efficacy of the antimicrobial properties. It should be noted that reagents should not be stored with other chemicals that could cause contamination.

### **Place Exchange Reactions**

Place-exchange reactions were performed to swap various pMBA molecules with thiol ligands of interest on the surface of the gold nanoparticles. One-pot place-exchange reactions were conducted with  $7.4 \mu\text{M}$  gold nanoparticles in 4 mL of sterilized 20 mM  $\text{Na}_2\text{HPO}_4$  pH 9.5 in 15 mL conical centrifuge tubes. The thiol ligands were then added to the gold nanoparticles in specific molar feed ratios. The nanoparticles used as the foundation of this experiment utilized thiols 5, 8, and 9 in 33x molar excess of the gold nanoparticles. Thiol-6 was utilized at 46x molar excess and thiol-11 was used in 16.5x molar excess. These are the feed ratios utilized in the exchange reactions unless otherwise specified. The thiols were stored at  $-80^\circ\text{C}$  at 20 mM in water, except for thiol 11, which was stored in DMSO. The solutions of gold, thiol ligands and  $\text{Na}_2\text{HPO}_4$  were mixed and agitated on a plate shaker for 24 hours at  $19^\circ\text{C}$ .

The exchanged product was harvested through the addition of 2 mL of 5.0 M NaCl and 9 mL of methanol. The conical tubes were then centrifuged at 3200x g for 20 minutes. The supernatant was discarded, and the pellet was re-suspended in 4-6 drops of filter-sterilized ultrapure  $\text{H}_2\text{O}$ . The nanoparticles were then precipitated again by the addition of 500  $\mu\text{L}$  of 5.0 M NaCl and 8 mL of methanol to each hydrated pellet, followed by centrifugation at 3200x g for 10 minutes. After discarding the supernatant,

the pellet was allowed to dry to completion overnight.

After 24 hours, the pellet was re-suspended in filter-sterilized ultrapure water, before being washed over a 10k M.W.C.O. filter (Millipore) to remove excess salt and free thiol ligands. The particles were washed eight times for 4 minutes at 12,000x g. Particle concentration was determined through UV-visible spectroscopy ( $\epsilon_{510\text{nm}} = 409,440 \text{ M}^{-1}\text{cm}^{-1}$ ).

### **Growth Inhibition Assay**

All bacterial experimentation was performed in a SterilGard III Advance<sup>0</sup> Class II Biological Safety Cabinet to drastically decrease the potential of contamination. Cultures of the bacteria were generated by touching the top of four well-isolated colonies of the bacteria of interest from an agar plate with a pipette tip and grown in 3 mL of broth. The bacteria utilized in this experiment were *Escherichia coli* (ATCC 25922), which had been grown in Mueller-Hinton broth (Fisher); *Klebsiella pneumoniae* (ATCC BAA 2146), grown in Mueller-Hinton II cation-adjusted media (Fisher); *Mycobacterium avium* (MAC 104WT); and *Mycobacterium abscessus* (ATCC 19977), grown in Middlebrook 7H9 Broth (Fisher).

Cultures were grown at 37°C and 225 rpm, until visible turbidity was reached. The initial culture incubation period was 4 hours for *E. coli*, 12 hours for *K. pneumoniae*, 24 hours for *M. abscessus*, and 72 hours for *M. avium*. After the incubation period, the bacteria cultures were diluted to  $2 \times 10^6$  CFU/mL. The bacterial concentration was determined using UV-Visible Spectroscopy where an  $\text{OD}_{600}$  of 0.001 is assumed to be approximately  $1 \times 10^6$  CFU/mL. The nanoparticle samples were diluted to the desired testing concentration with the correct broth for the specific bacterium. Equal volumes of

nanoparticle and inoculation sample were mixed, which made the final bacteria concentration  $1 \times 10^6$  CFU/mL. Samples were then incubated at 37°C and 225 rpm. The growth inhibition incubation times were 18 hours for *E. coli*, 24 hours for *K. pneumoniae*, 72 hours for *M. abscessus*, and 168 hours for *M. avium*.

Percent inhibition was determined by serially diluting cultures in 1x PBS and plating on Mueller-Hinton agar plates for *E. coli*, Mueller-Hinton II plates for *K. pneumoniae*, and Middlebrook 7H10 agar plates for *M. abscessus* and *M. avium*. The plates were incubated at 37°C for the same amount of time as the growth inhibition incubation times indicated for the specific bacterium. The MIC<sub>99.9</sub> was defined as the minimum nanoparticle concentration that inhibits 99.9% of bacterial growth, which was determined by colony counting.

### **Resistance Assays**

A resistance assay was performed with varying gold nanoparticle conjugates. An overnight culture of *Klebsiella pneumoniae* (ATCC BAA 2146) was grown by touching the tops of four well-isolated colonies of bacteria with a pipet tip from a plate of Mueller-Hinton II agar and grown in 3 mL of Mueller-Hinton II broth. This culture was allowed to grow for 24 hours before being diluted to  $2 \times 10^6$  CFU/ mL in Mueller-Hinton II broth. The nanoparticles of interest were diluted in Mueller-Hinton II broth so that  $1 \times 10^6$  CFU/mL of bacteria would be incubated in the final volume with 60% of the MIC<sub>99.9</sub>. Equal volumes of nanoparticle and bacteria were combined and incubated at 37°C and 225 rpm. The same sample of bacteria was serially passed every 24 hours by taking 5 µL of bacteria and adding it to 500 µL of fresh broth with an additional treatment of 60% of the MIC<sub>99.9</sub> of nanoparticle.

pMBA-capped nanoparticles were serially passed to determine if the bacteria continually exposed to the pMBA-capped conjugates remained sensitive to the active conjugates. The pMBA-capped nanoparticles were found to have no antimicrobial properties at any concentration tested (up to 50  $\mu\text{M}$ )<sup>1</sup>, and therefore do not have an  $\text{MIC}_{99.9}$ . As a consequence, it was arbitrarily assigned that 10  $\mu\text{M}$  of the pMBA would be passed every 24 hours. A bacteria-only (no nanoparticle treatment) negative control was also carried through the passages.

The minimum inhibitory concentration was tested at various times during the resistance assay to monitor the  $\text{MIC}_{99.9}$  of the nanoparticle compounds. Bacterial resistance to the nanoparticle conjugates was defined as an increase in the  $\text{MIC}_{99.9}$  to 10x the original  $\text{MIC}_{99.9}$ . The lower concentrations tested (1x, 2x, and 5x  $\text{MIC}_{99.9}$ ) also had to fail to produce 99.9% inhibition for resistance to be confirmed, thus ruling out experimental error.

### **Gene Expression Profiling**

A 4 mL overnight culture of *K. pneumoniae* (ATCC BAA 2146) was diluted into 75 mL of Mueller-Hinton II broth, and grown to  $\text{OD}_{600} = 0.7$ . The bacteria culture was divided into fifteen 4 mL cultures, in 25 mL Erlenmeyer flasks. An additional 2 mL of Mueller-Hinton II broth was added to each culture. The three active nanoparticle conjugates tested and pMBA-capped gold nanoparticles (all repeated in triplicate) were added to a final concentration of 6.25  $\mu\text{M}$ . “Bacteria only” (containing no nanoparticle conjugate) controls were also run in triplicate. The samples were incubated at 37°C and 225 rpm for 4 hours, and then 2 mL of each sample were used for RNA extraction.

The nanoparticle conjugate samples were washed with 1x PBS, followed by centrifugation at 3200x g for 2 minutes to remove the nanoparticle conjugates from the cell pellet. Total RNA was extracted from the samples using the Bio-Rad Aurum Total RNA Mini-Kit. RNA extraction was confirmed by running the samples on a 1.0% TBE agarose gel, and then visualized by ethidium bromide staining. A Quick-Load 2-Log DNA Ladder (0.1 – 10.0 kb) (New England Biolabs) was used to check the presence of the 16s and 23s rRNA bands. The quality of RNA was confirmed using an Agilent 2100 Bioanalyzer and Agilent RNA 6000 Nano Chips at the Next-Generation Sequencing Facility, Biofrontiers Institute of the University of Colorado. The total RNA samples were then frozen and shipped on ice to BGI Americas Corporation (Cambridge, MA) for mRNA isolation and RNA-Seq Transcriptome Resequencing.

BGI first removed rRNA, then fragmented the mRNA, and finally synthesized the cDNA using the mRNA as a template. The suitable fragments were amplified using Polymerase Chain Reaction (PCR) and sequenced with an Illumina HiSeq<sup>TM</sup> 2000 sequencing platform with single-end 50 bp reads. The sequences data was aligned with the reference sequence using SOAPaligner/SOAP2. Bioinformatics, including a differential gene expression analysis, Gene Ontology (GO) enrichment analysis, and pathway enrichment analysis was performed by BGI Americas Corporation.

## Bibliography

[1] Bresee, J.; Bond, C. M.; Worthington, R. J.; Smith, C. A.; Gifford, J. C.; Simpson, C. A.; Carter, C. J.; Wang, G.; Hartman, J.; Osbaugh, N. A.; Shoemaker, R. K.; Melander, C.; Feldheim, D. L. *J. Am. Chem. Soc.* **2014**, *136*, 5295–5300.

### III. Results and Discussion

#### Discovering Gold Nanoparticle Conjugates Active Toward *K. pneumoniae*

This honors project aimed at finding gold nanoparticle conjugates that were effective inhibitors against *Klebsiella pneumoniae* (ATCC BAA 2146). Nanoparticle conjugates previously found by the Feldheim Lab to be potent inhibitors of *Escherichia coli* (ATCC 25922) growth were initially tested as candidates. Because both strains of bacteria are Gram-negative members of the *Enterobacteriaceae* family, their responses to antibiotics were likely to be similar. The main differences between the two bacteria species is the thick coat of extracellular polysaccharide of *Klebsiella pneumoniae* called a “capsule” that helps protect the cells from desiccation and phagocytosis when inside an animal host.<sup>1</sup> The capsule that *K. pneumoniae* produces has been shown to provide resistance to antimicrobial peptides and proteins, and reduces cell membrane penetration by some antibiotics.<sup>2,3</sup> This specific strain of *K. pneumoniae* also expresses New Delhi Metallo- $\beta$ -lactamase (NDM-1), an enzyme that confers resistance to beta-lactam antibiotics including last-resort Carbapenems.<sup>4</sup> The NDM-1 is encoded by the *bla<sub>NDM</sub>* gene (associated with a plasmid) and is transmissible through horizontal gene transfer.<sup>5</sup> The *E. coli* strain primarily used in previous gold nanoparticle experiments displayed sensitivity to every type of antibiotic tested, including some beta-lactams.<sup>5</sup>

The high efficacy of conjugates LAL-32, LAL-33, LAL-42, and LAL-52 (Table 1.2) toward *E. coli* growth inhibition made them desirable candidates to be tested against *K. pneumoniae*. Experimentation found each of these four particles to be an effective inhibitor against *K. pneumoniae*, with a slightly increased Minimum Inhibitory

Concentration ( $MIC_{99.9}$ ) that reduced bacterial growth by 99.9%. Table 2.1 reports the  $MIC_{99.9}$  for the tested nanoparticles for both *E. coli*<sup>6</sup> and *K. pneumoniae*.

**Table 2.1:  $MIC_{99.9}$  values for various gold nanoparticle conjugates against *E. coli* and *K. pneumoniae* as determined by colony counting.** *E. coli*  $MIC_{99.9}$  values reported from *J. Am. Chem. Soc.* 2014, 136, 5295–5300.

Nanoparticle Conjugate	$MIC_{99.9}$ ( <i>E. coli</i> ) $\mu M^6$	$MIC_{99.9}$ ( <i>K. pneumoniae</i> ) $\mu M$
LAL- 32	0.25	0.625
LAL- 33	0.5	1.25
LAL- 42	0.5	1.25
LAL- 52	0.25	0.625

The efficacy of the gold nanoparticles conjugate depends on precise synthesis, including the integrity of the chemical agents. In addition, the percent inhibition of the conjugates varies slightly between batches. The reported  $MIC_{99.9}$  values in Table 2.1 were found to consistently inhibit at least 99.9% of bacterial growth.

### **Altering the Active Conjugate to Increase *K. pneumoniae* Growth Inhibition**

LAL-32 consisted of ligands 5, 6, and 8 (Table 1.1) with feed ratios of 33x, 46x, and 33x respectively. LAL-52 contained ligands 5, 6, and 11 with feed ratios of 33x, 46x, and 16.5x respectively. These two conjugates were found to be the most effective inhibitors of *K. pneumoniae*. The Feldheim Lab previously proved that the antimicrobial activity of the gold nanoparticle conjugates was dependent on the feed ratio of the various ligands in the monolayer.<sup>6</sup> Therefore, it was hypothesized that altering the feed ratios of one of the existing *E. coli* conjugates could produce a more active nanoparticle against *Klebsiella pneumoniae*.

LAL-32 was chosen as the conjugate to be altered in this experiment due to the lower MIC<sub>99,9</sub>, which indicated a higher efficacy of inhibition, as well as the relatively easy obtainment of ligand 8 compared to ligand 11 in high quantities. The search for optimizing feed ratios began by multiplying the existing feed ratios (33x, 46x, 33x) of one or two of the ligands by factors such as 0.75 or 1.25, and testing the resulting conjugate for activity. The subsequent conjugates were tested against *K. pneumoniae* at 0.625 μM and 1.25 μM. Presumably, if the MIC<sub>99,9</sub> increased by more than 2-fold, the altered feed-ratio conjugate would not be an improvement over the original formulation, and therefore should not be kept as a *K. pneumoniae* inhibitor candidate.

The nanoparticle-exposed bacterial cultures were analyzed visually for turbidity after 24 hours. Plating and colony counting were utilized to determine the logs of inhibition if the cultures were found to be clear. The logs of inhibition were determined using the formula:

$$\text{Log} \left( \frac{\text{Colony Forming Units with treatment}}{\text{Colony Forming Units with no treatment}} \right)$$

where 3 logs of inhibition is equal to 99.9%, 4 logs of inhibition = 99.99%, etc.

Table 2.2 illustrates the results obtained from the altered feed ratio experiment.

**Table 2.2 : The Feed Ratio of thiol ligands in the altered feed ratio conjugates, the resulting turbidity at 0.625  $\mu$ M and 1.25  $\mu$ M, as well as the logs of inhibition at 0.625  $\mu$ M if applicable. Error in the logs of inhibition was calculated by plating and colony counting in triplicate and calculating the standard deviation**

Gold Nanoparticle Conjugate	Feed Ratio of 5	Feed Ratio of 6	Feed Ratio of 8	Turbidity at 0.625 $\mu$ M	Turbidity at 1.25 $\mu$ M	Logs of Inhibition at 0.625 $\mu$ M
LAL-32	33	46	33	clear	clear	3.45 $\pm$ 0.36
LAL-32 a	16.5	46	33	turbid	turbid	n/a
LAL-32 b	33	23	33	turbid	turbid	n/a
LAL-32 c	33	46	16.5	clear	clear	3.17 $\pm$ 0.31
LAL-32 d	41.25	33	46	turbid	turbid	n/a
LAL-32 e	49.5	33	46	clear	clear	4.14 $\pm$ 0.48
LAL-32 f	33	33	57.5	turbid	clear	n/a
LAL-32 g	33	33	69	clear	clear	4.66 $\pm$ 0.52
LAL-32 h	33	41.25	46	turbid	turbid	n/a
LAL-32 i	33	49.5	46	turbid	turbid	n/a
LAL-32 j	33	33	33	clear	clear	4.53 $\pm$ 0.42
LAL-32 k	46	46	46	clear	clear	3.51 $\pm$ 0.47
LAL-32 L	49.5	46	33	clear	clear	1.90 $\pm$ 0.12
LAL-32 m	33	69	33	turbid	turbid	n/a
LAL-32 n	33	46	49.5	turbid	turbid	n/a

Three altered feed ratio conjugates, LAL-32 e, LAL-32 g and LAL-32 j, were found to inhibit the growth of *K. pneumoniae* more effectively than the original LAL-32 conjugate, and were therefore selected for further testing. Serial dilutions ranging from 20  $\mu$ M to 0.04  $\mu$ M of the conjugates were incubated with the bacteria to test for the MIC<sub>99.9</sub>. Table 2.3 reports the logs of inhibition determined by plating and colony counting for selected concentrations near the transition from turbid to clear for the bacterial cultures.

**Table 2.3: The logs of inhibition for selected gold nanoparticle conjugates at 0.313  $\mu\text{M}$ , 0.625  $\mu\text{M}$ , and 1.25  $\mu\text{M}$ , as determined by plating and colony count.** Error in the logs of inhibition was calculated by plating and colony counting in triplicate and calculating the standard deviation.

<b>Nanoparticle Conjugate</b>	<b>Logs of Inhibition at 0.313 <math>\mu\text{M}</math></b>	<b>Logs of Inhibition at 0.625 <math>\mu\text{M}</math></b>	<b>Logs of Inhibition at 1.25 <math>\mu\text{M}</math></b>
LAL-32	2.87 $\pm$ 0.29	3.45 $\pm$ 0.36	3.74 $\pm$ 0.38
LAL-32 e	2.74 $\pm$ 0.37	4.14 $\pm$ 0.48	4.53 $\pm$ 0.23
LAL-32 g	1.89 $\pm$ 0.21	4.66 $\pm$ 0.52	7.66 $\pm$ 0.56
LAL-32 j	2.16 $\pm$ 0.25	4.53 $\pm$ 0.42	7.50 $\pm$ 0.47

Experimentation revealed that conjugates LAL-32 g and LAL-32 j were capable of inhibiting approximately seven logs of inhibition at the concentrations tested. LAL-32 and LAL-32 e did not appear to reach that efficacy of inhibition at any concentration tested. It should be noted that at high concentrations (above 12  $\mu\text{M}$ ), the nanoparticles appeared to lose efficacy and the cultures were turbid. This phenomenon may be due to aggregation of the nanoparticles in the nutrient broth.

The Feldheim Lab defines nanoparticles that inhibit more than 5 logs or 99.999% growth versus the untreated control to be bactericidal, making conjugates LAL-32 g and LAL-32 j bactericidal compounds.<sup>7</sup> Bactericidal antibiotics are defined by the ability to kill microbes, while bacteriostatic antibiotics inhibit growth.<sup>8</sup> Experimentation suggests that LAL-32 g and LAL-32 j become bactericidal at higher concentrations, while LAL-32 and LAL-32 e remain bacteriostatic at all concentrations. Table 2.4 reports the defined  $\text{MIC}_{99.9}$  and the Minimum Bactericidal Concentration (MBC) for conjugates LAL-32, LAL-32 e, LAL-32 g, and LAL-32 j.

**Table 2.4: The defined MIC<sub>99.9</sub> and MBC for selected gold nanoparticle conjugates.**

<b>Nanoparticle Conjugate</b>	<b>MIC<sub>99.9</sub></b>	<b>MBC</b>
LAL-32	0.625 μM	n/a
LAL-32 e	0.625 μM	n/a
LAL-32 g	0.625 μM	1.25 μM
LAL-32 j	0.625 μM	1.25 μM

This experiment showed that altering the feed ratio of the thiol ligands in the monolayer of a gold nanoparticle could drastically alter the inhibitory efficacy, and change a bacteriostatic conjugate into a bactericidal conjugate.

#### **Determining the Time to Resistance for *K. pneumoniae***

A resistance assay was performed on the *K. pneumoniae* bacteria to investigate how the altered feed ratio conjugates would affect the time to resistance. The bacteria were incubated with 60% of the MIC<sub>99.9</sub> and serially passed until resistance was achieved. Resistance was defined when the MIC<sub>99.9</sub> was increased to 10 times the original MIC<sub>99.9</sub>. All lower concentrations tested must have also failed to produce 99.9% inhibition for resistance to be confirmed.

The nanoparticle conjugates selected for resistance testing were LAL-52, LAL-32, LAL-32 g, and LAL-32 j due to high antimicrobial efficacy. Resistance assays were also conducted on two different antimicrobial treatments that were alternated every 24 hours to determine if rotating exposures could help extend the time to resistance. Treatments of LAL-52 and LAL-32 were alternated every day to determine the time to resistance of alternating exposures. In a separate trial, treatments of LAL-32 g and LAL-32 j were also alternated every day. The pMBA-capped nanoparticles were passed alongside the active conjugates to determine if the bacteria continually exposed to the

gold core would remain sensitive to the active conjugates. The results of the resistance assay are presented in figure 2.1.

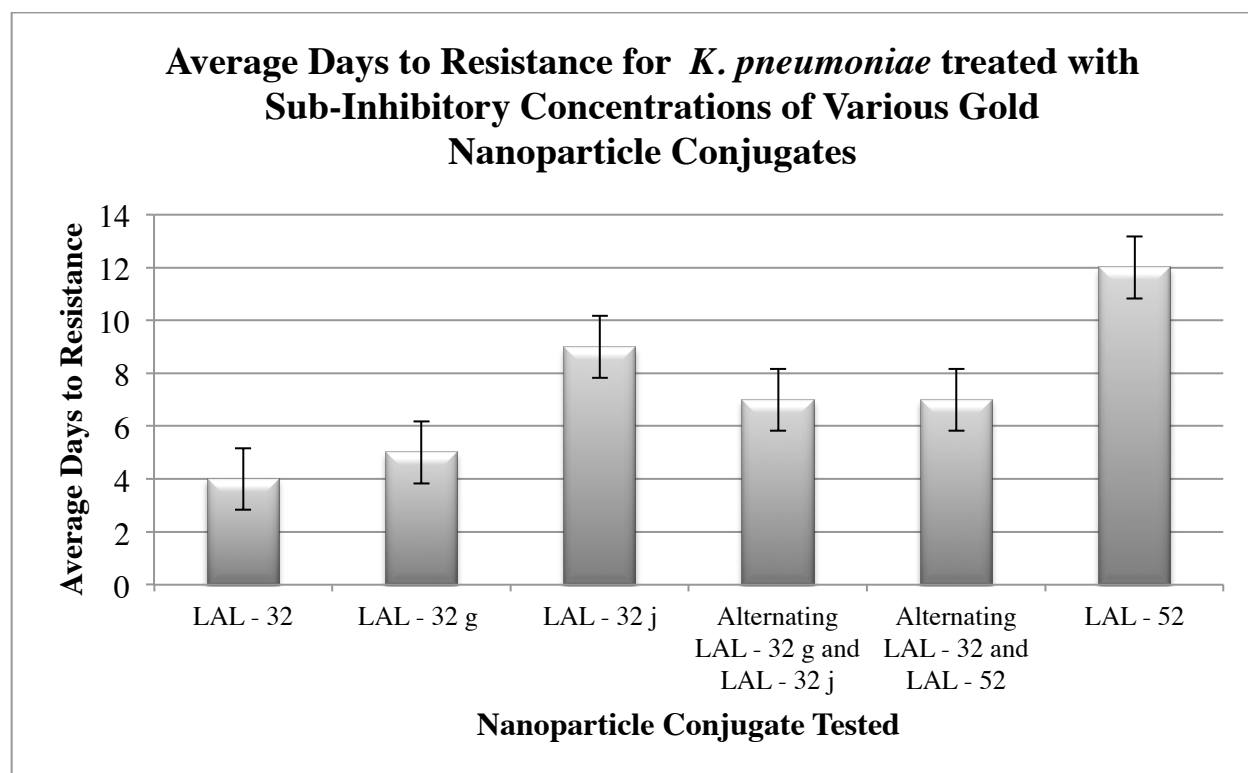


**Figure 2.1:** The average days to resistance for *K. pneumoniae* treated with 60% of the MIC<sub>99.9</sub> of various gold nanoparticle conjugates. The average days to resistance were calculated based on two different resistance assays and the error bars represent the upper and lower limits of the two resistance assays.

*K. pneumoniae* developed resistance to the original LAL-32 compound at a fairly quick rate (4 days). The LAL-32 g and LAL-32 j compounds both increased the time to resistance over the original compound LAL-32. LAL-32 j increased the time to resistance more than 2-fold over the original compound. By alternating between two different compounds, an intermediate time to resistance was produced. The bacteria were sensitive to conjugate LAL-52 for the longest duration, having a three-fold increase in time to resistance over LAL-32. The single difference between LAL-32 and LAL-52 was the exchange of ligand 8 for ligand 11. This exchange indicated that the thiol ligands in the

monolayer of the gold nanoparticle conjugates altered the time to resistance significantly. Therefore, the conjugates could potentially be improved to further avoid antibiotic resistance.

Bacteria that were serially passed in the presence of the pMBA-capped gold nanoparticles for 12 days remained sensitive to the active conjugates. The experimental evidence showed that the bacteria did not become resistant to the gold core, but did become resistant to the mixed monolayer active conjugates. Furthermore, the bacteria that were resistant to one conjugate of nanoparticle were also resistant to all variants tested. Once resistance was activated, cellular adjustments within the bacterium conferred resistance to the various *K. pneumoniae* active conjugates, suggesting a similar mode of action for LAL-52 and LAL-32, as well as the altered feed ratio variants.

The original conjugate LAL-32 with feed ratios of 33x, 46x, 33x for ligands 5, 6, 8 respectively had an MIC<sub>99,9</sub> of 0.625 μM and a time to resistance of 4 days. Decreasing the feed ratio of ligand 6 to 33x produced conjugate LAL-32 j, which was bactericidal at 1.25 μM and doubled the time to resistance. Exchanging ligand 8 of LAL-32 for ligand 11 produced LAL-52, which tripled the time to resistance. This experiment showed that both the identity and feed ratio of the thiol ligands significantly altered the antimicrobial effect of the conjugate, and the time to resistance.

### **Differential Gene Expression Experiment**

A differential gene expression experiment was performed to determine how the varying nanoparticle conjugates were affecting *K. pneumoniae*, and possibly further elucidate the mode of action of the gold nanoparticles. Analyzing the most altered genetic pathways by the nanoparticles may indicate how the conjugates were inhibiting bacterial growth. Samples of bacteria were incubated with conjugates LAL-32, LAL-32 j and LAL-52, as well as the pMBA-only capped conjugates. The inactive starting material control was utilized to investigate the impact of the gold core on the bacteria. An untreated bacteria control was utilized as a negative control to determine which genes were differentially expressed upon exposure to the gold nanoparticles.

The bacteria were incubated for adequate time for the conjugates to be internalized into the cell, while remaining within the exponential growth phase. Total RNA was extracted from the samples and sent to BGI Americas for RNA-Sequencing and bioinformatics. The differential gene expression analysis examined the quantity of each gene expressed in the conjugate-exposed samples compared to the bacteria-only control. This analysis also assessed the gene expression levels in the active conjugate-exposed samples compared to the pMBA-only control sample. Figure 2.2 shows the number of genes differentially expressed in each comparison.

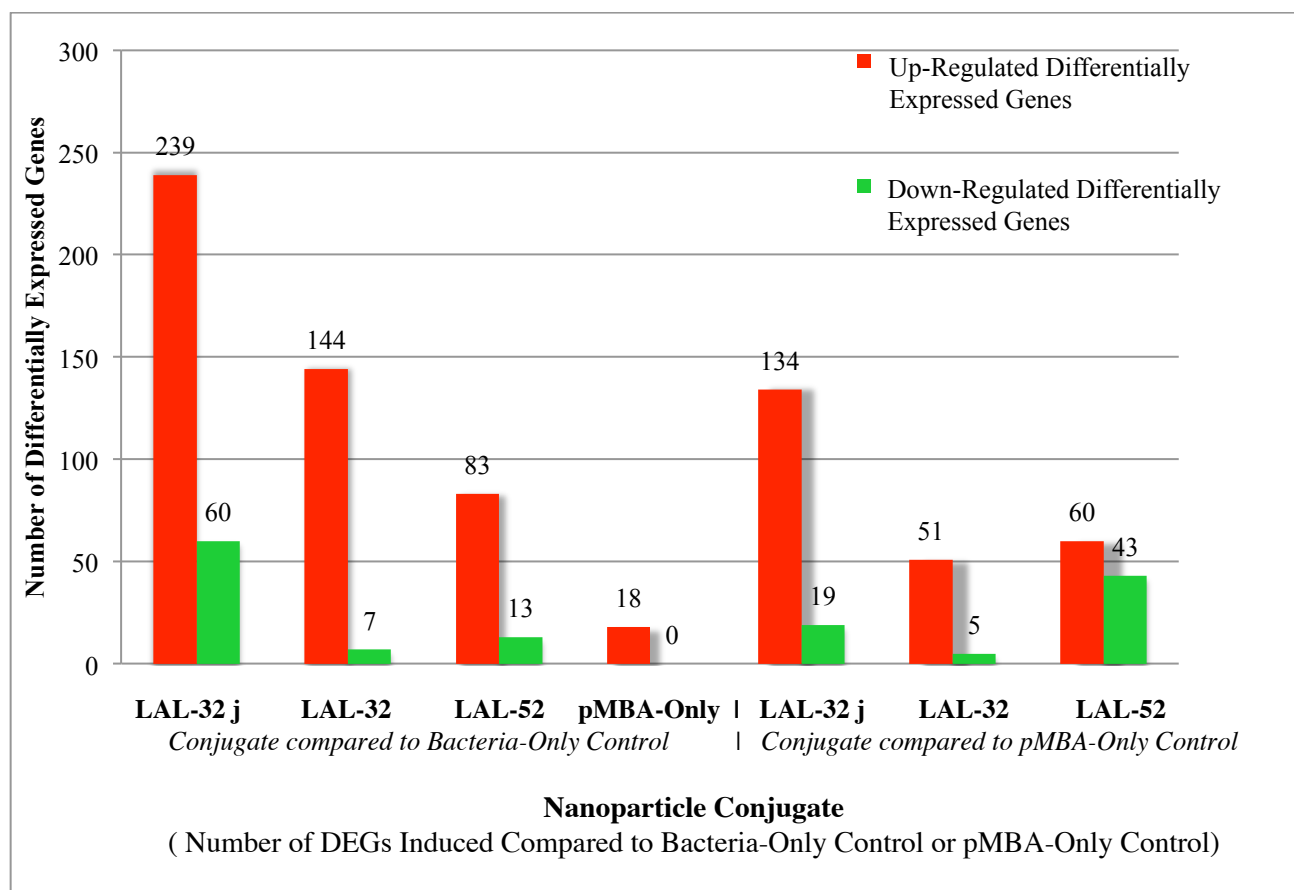


**Figure 2.2: The Number of Differentially Expressed Genes For LAL-32, LAL-32 j, and LAL-52 Gold Nanoparticle Conjugates Compared to a Bacteria-Only Control (No Treatment) as well as a pMBA-Only Gold Nanoparticle Control**

**\*Note:** The reported differentially expressed genes (DEGs) have a False Discovery Rate (FDR)  $\leq 0.001$  and a  $|\log_2 \text{Ratio}| \geq 1$  and are reported as statistically significant by BGI Americas. Figure from BGI Transcriptome Resequencing Report.

Figure 2.2 shows that exposure to LAL-32 j up-regulated 239 genes in *K. pneumoniae*, whereas only 144 and 83 genes were up-regulated upon exposure to the LAL-32 and LAL-52 conjugates respectively. The gene expression analysis demonstrated the LAL-32 j conjugate affected gene expression in the bacteria significantly more than the original LAL-32 conjugate. Eighteen genes were affected by the pMBA-only inactive control particles, which suggested that the mixed thiol-ligand monolayer affected the majority of the differentially expressed genes.

### **Analysis of the Differentially Expressed Genes**

An extensive analysis was performed to determine how the nanoparticles were affecting the bacteria. In summary, a pathway analysis was performed to broadly determine which pathways were most affected by the nanoparticles. A Process Ontology evaluation was then performed to closely analyze some of the select pathways. The individual genes with the most differential expression were then examined to further analyze how the nanoparticles were altering gene expression. Genes that were common to all four nanoparticles, common to only the three active conjugates, as well as genes unique to LAL-32 j are discussed in this manuscript.

## A. Pathway Analysis of the Differentially Expressed Genes

A pathway analysis was performed to determine which biological pathways were most affected by the gold nanoparticles. Table 2.5 reports the pathways with the most significant quantity of differentially expressed genes (DEGs).

**Table 2.5: The Number of Differentially Expressed Genes (DEGs) Related to Select Biological Pathways Upon Exposure to Gold Nanoparticle Conjugates**

\*Note: This is not a complete list of the differentially expressed genes. Pathways selected for reporting had a large alteration or were of biological interest. An absolute value of  $\text{Log}_2\text{Ratio} \geq 1$  was utilized as the threshold to judge the significance of differential gene expression. DEGs may exist within multiple categories.

Pathway	DEGs with LAL-32 j / Bacteria-Only (Percentage out of 209 total)	DEGs with LAL-32/ Bacteria-Only (Percentage out of 117 total)	DEGs with LAL-52/ Bacteria-Only (Percentage out of 80 total)	DEGs with pMBA-Only/ Bacteria-Only (Percentage out of 14 total)
Metabolic Pathways	47 (22.49%)	32 (27.35%)	15 (18.75%)	6 (42.86%)
Biosynthesis of Secondary Metabolites	30 (14.35%)	17 (14.53%)	11 (13.75%)	6 (42.86%)
ABC Transporters	12 (5.74%)	7 (5.98%)	4 (5%)	0
Phenylalanine Metabolism	11 (5.29%)	12(10.26%)	8 (10%)	0
Tyrosine Metabolism	9 (4.31%)	6 (14.29%)	8 (10.39%)	1 (7.14%)
Two Component System	8 (3.38%)	1 (0.85%)	4 (5%)	0
Ribosome	7 (3.35%)	10 (8.55%)	6 (7.5%)	1 (7.14%)
Glycolysis/ Gluconeogenesis	7 (3.35%)	4 (3.42%)	1 (1.25%)	2 (14.29%)
Citrate Cycle (TCA)	5 (2.39%)	6 (5.13%)	0	5 (35.71%)
Histidine Metabolism	0	0	4 (5.19%)	0

The results in Table 2.5 indicated that the nanoparticles affected pathways relating to the biosynthesis of secondary metabolites and metabolism most significantly. Secondary metabolites are not directly involved in the normal growth or development of bacterial cells; however, they are usually produced in the late growth phase, and often

have antibiotic, pathogenic, or cellular differentiation properties.<sup>9</sup> Metabolism includes all chemical reactions utilized to extract, convert and store energy from nutrients. The metabolic pathways were the most altered and were therefore selected for further analysis.

### I. Initial Metabolic Pathway Analysis Based on Ligand Structure

Some of the thiol ligands were chosen in part due to their similar structure to amino acids. Ligand 5 is glutathione, a tripeptide, ligand 6 is a degradation product of cysteine, and ligand 11 is a thiolated histidine with a short polyethylene glycol linker. Phenylalanine and Tyrosine metabolism were both notably up-regulated by each of the active gold-nanoparticle conjugates. Figure 2.3 shows the similar structure between the pMBA molecule in the monolayer and the amino acids.

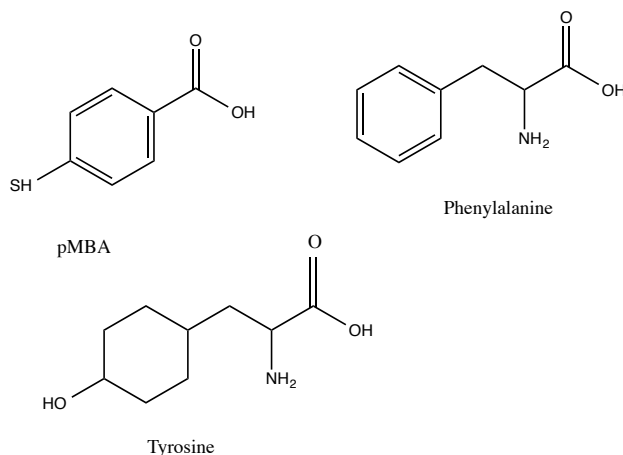


**Figure 2.3 The Structures of pMBA, Phenylalanine, and Tyrosine**

This large influx of amino-acid-like structures may have influenced the bacteria's metabolism. LAL-52 contained the thiolated-histidine molecule, and was the only conjugate to up-regulate histidine metabolism.

These amino-acid ligands may also mimic protein-protein interactions. Many transient protein complexes resemble receptor-ligand interactions, and are mediated by

protein interaction modules binding to short peptides exposed on the surface of target proteins.<sup>10</sup> The interaction site and the target peptide are usually small. The nanoparticles may allow for competitive disruption of the complex and repression of the protein function.<sup>10</sup> The bacteria may up-regulate metabolism in order to overcome the decrease in protein function.

## **II. Initial Metabolic Pathway Analysis Based on Cell Stress**

There is a possibility that the nanoparticles were causing environmental stress to the bacterial cells. It has been shown that antimicrobials cause a significant environmental impact on bacteria, which affect a variety of adaptive and protective responses. Bacteria modulate their gene expression patterns in response to environmental cues that allow the cells to adapt and survive. This modulation requires sensors to detect chemical or physical signals, and regulators to bring about changes in the levels of gene products, often in the form of a Two-Component Regulatory System.<sup>11</sup> Table 2.5 reports that each active conjugate affected Two-Component Systems, which indicated that the bacteria were altering gene expression in response to environmental changes. The Two Component System Pathways were unaltered by the pMBA-only conjugates. This suggests that the presence of the gold-core in solution was not stimulating the adaptive changes in the bacteria; however, the antimicrobial active gold nanoparticle conjugates initiated the gene expression changes for survival.

Common adaptations as a result of environmental stress often include growth cessation or dormancy, changes to antimicrobial targets, alterations to the membrane barrier functions, generation of resistance mutations, or promotion of resistant growth modes, such as biofilms.<sup>12</sup> The cells adjust to environmental changes by altering their

metabolism systematically.<sup>11</sup> Metabolism includes a wide range of chemical processes, which is why a process ontology analysis was conducted to further examine the effects of the gold nanoparticles.

### **B. Process Ontology to Further Analyze Metabolism Pathways**

A Process Ontology analysis was performed to more closely examine the biological processes affected by the nanoparticles. Table 2.6 lists the number of differentially expressed genes related to select biological processes.

**Table 2.6: The Number of Differentially Expressed Genes (DEGs) Related to Select Biological Processes Upon Exposure to Gold Nanoparticle Conjugates**

\*Note: This is not a complete list of the differentially expressed genes. Processes selected for reporting had a large alteration or were of biological interest. An absolute value of  $\text{Log}_2\text{Ratio} \geq 1$  was utilized as the threshold to judge the significance of differential gene expression.

<b>Process</b>	<b>Number of DEGs Related to Process LAL-32 j / Bacteria-Only (165 total)</b>	<b>Number of DEGs Related to Process LAL-32/ Bacteria-Only (93 total)</b>	<b>Number of DEGs Related to Process LAL-52/ Bacteria-Only (66 total )</b>
Metabolic Process	114	75	54
Biosynthetic Process	36	25	27
Oxidation Reduction Process	33	25	20
Regulation of Biological Processes	28	10	4
Transport	25	13	9
Response to Stress	14	8	0
Cellular Component Biogenesis	9	5	4
Cell Division	6	2	0
Response to Antibiotic	5	0	6
Translation	5	9	5
Cell Cycle	4	0	0
Electron Transport Chain	3	0	2
Cytokinesis	3	0	0
Septum Assembly	2	0	0

The process ontology analysis confirmed that the majority of the DEGs were related to metabolic functions. However, it should be noted that many of the DEGs exist within multiple categories; numerous processes listed are sub-categories of metabolism. Figure 2.4 illustrates the biosynthetic processes and the oxidative reduction processes fall within the metabolic process category for the DEGs induced with exposure to LAL-32 j.

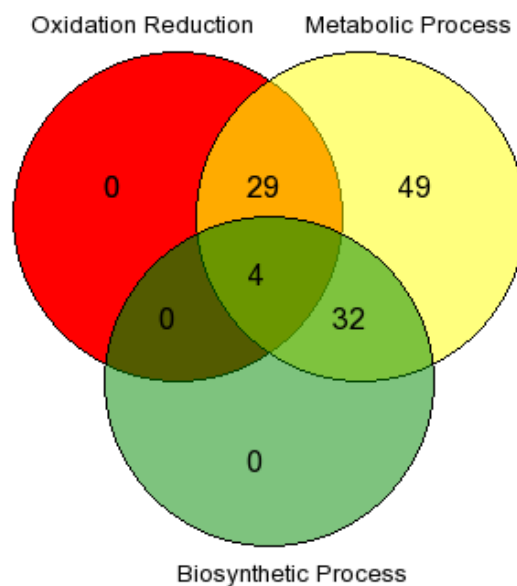


**Figure 2.4 A venn diagram of the three major processes affected by DEGs in *K. pneumoniae* upon exposure to LAL -32 j compared to the bacteria-only control**

The three gold nanoparticle conjugates all appeared to affect a wide variety of metabolic pathways, but further analysis indicated that the metabolic changes were not identical with exposure to the different nanoparticle conjugates. When the differentially expressed genes in the metabolic process category from each active conjugate were compared, there was significant variation. Figure 2.5 shows the DEGs in the metabolic

process category induced upon exposure to the three different active gold nanoparticle conjugates.

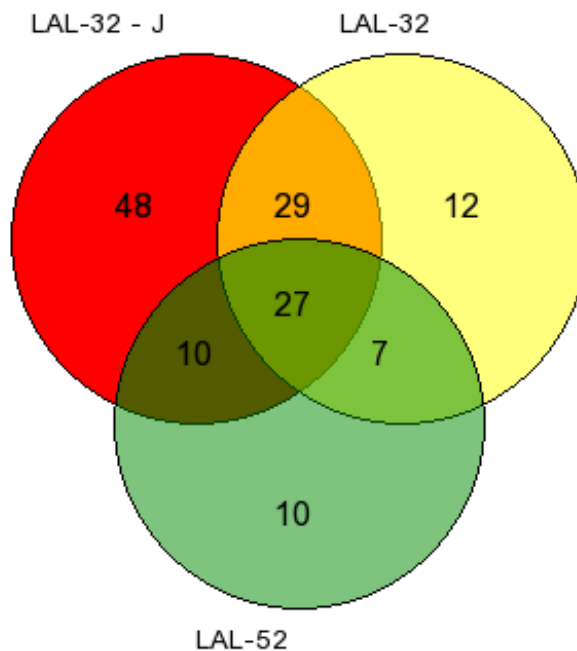


**Figure 2.5: A venn diagram comparing the DEGs in the metabolic category induced upon exposure to the three different active gold nanoparticle conjugates.**

Although the pathway ontology data suggested that each gold nanoparticle significantly affected the metabolism of *K. pneumoniae*, Figure 2.5 illustrates the effects on metabolism vary with each conjugate. The primary conclusions drawn from the Process Ontology report indicated that the biosynthetic processes, oxidation-reduction processes, transport, and regulation of biological processes were the main sub-category pathways affected by all nanoparticles.

The data also indicated the expression of genes related to cell division were altered by LAL-32 j, but not LAL-32. LAL-32 j had the highest efficacy of inhibition out of the three conjugates and became bactericidal at 1.25  $\mu\text{M}$ . This suggests that higher

efficacy nanoparticles may alter cell division more than nanoparticle conjugates with less antimicrobial efficacy.

### **C. Individual DEG Analysis**

In order to better understand how the different nanoparticle conjugates were affecting the biological pathways, the individual genes with the highest levels of differentiation were analyzed. An absolute value of  $\text{Log}_2(\text{gene expression with treatment} / \text{gene expression no treatment}) \geq 1$  was considered a statistically significant alteration in gene expression, and these genes were included in the pathway and process ontology analyses. However, for the individual gene analysis, DEGS with a  $\text{Log}_2(\text{treatment} / \text{control}) \geq 2$  were selected in order to determine which genes had the most altered expression upon exposure to all of the gold nanoparticles. Table 2.7 lists DEGs with a  $\text{Log}_2(\text{treatment} / \text{control}) \geq 2$  that were common to all of the gold-nanoparticle conjugates or all of the active conjugates.

**Table 2.7: The Identification, Amount of Differentiated Gene Expression, and the Gene Product for Select Differentially Expressed Genes for the Gold Nanoparticle Conjugates Versus the Bacteria-Only Control**

\*Note: This is not a complete list of the differentially expressed genes. Genes selected for reporting were common to all four nanoparticle conjugates or the three active conjugates and had a  $|\text{Log}_2(\text{Treatment}/\text{Control})| \geq 2$ . Some hypothetical proteins with no known function and  $|\text{Log}_2(\text{Treatment}/\text{Control})| \leq 3$  were emitted to minimize data size. The color scale aids in the identification of Up-Regulated (Red) and Down-Regulated (Green) genes.

Gene ID	Log <sub>2</sub> Ratio (pMBA-Only/Bacteria-Only)	Log <sub>2</sub> Ratio (LAL-32 j/Bacteria-Only)	Log <sub>2</sub> Ratio (LAL-32/Bacteria-Only)	Log <sub>2</sub> Ratio (LAL-52/Bacteria-Only)	Gene Product
kpn2146_RS06320	4.3292	6.4613	6.0517	5.5607	copper exporting ATPase
kpn2146_RS16625	2.0174	5.4407	5.0302	4.6385	MerR family transcriptional regulator
kpn2146_RS04600	1.7357	3.0565	2.5390	2.3954	multicopper oxidase
kpn2146_RS09700	1.2623	2.1074	2.0791	1.2273	membrane protein; OmpA; Porin
kpn2146_RS11060		4.4607	1.9399	3.1191	hypothetical protein - belongs to a family involved in Cell wall/membrane/envelope biogenesis
kpn2146_RS26690		4.0572	2.7144	2.0315	glycerol uptake facilitator GlpF
kpn2146_RS04105		4.0545	3.8617	2.7521	hypothetical protein - periplasmic protein induced by stress response via Cpx and BaeSR system
kpn2146_RS17280		3.7335	1.6698	2.2814	membrane protein
kpn2146_RS15405		3.3854	1.2197	1.9092	hypothetical protein
kpn2146_RS06995		3.2401	3.1854	2.4998	hypothetical protein
kpn2146_RS11370		3.0505	2.4586	2.2201	hypothetical protein
kpn2146_RS10405		3.0337	2.9017	2.2289	hypothetical protein
kpn2146_RS03410		3.0217	1.2218	1.6827	porin
kpn2146_RS09395		2.8932	1.9523	2.0411	lipoprotein chaperone
kpn2146_RS17190		2.7529	1.1743	1.4875	heat shock protein HtpX
kpn2146_RS12445		2.7345	2.8770	2.1903	enoyl-CoA hydratase
kpn2146_RS25775		2.5802	1.3769	2.0182	zinc/cadmium/mercury/lead-exporting ATPase
kpn2146_RS08735		2.5244	1.6200	1.2321	outer membrane protein X
kpn2146_RS17335		2.5224	1.9638	1.2818	zinc ABC transporter substrate-binding protein
kpn2146_RS12435		2.3846	2.4332	2.3369	phenylacetic acid degradation protein
kpn2146_RS12390		2.3739	2.1352	1.6006	aldehyde dehydrogenase
kpn2146_RS25545		2.3341	1.8734	1.1519	glycerol-3-phosphate dehydrogenase
kpn2146_RS12420		2.2712	1.6891	2.3235	phenylacetate-CoA oxygenase subunit PaaB
kpn2146_RS21520		2.2490	1.0193	1.3690	iron ABC transporter substrate-binding protein
kpn2146_RS00385		2.2044	1.1839	1.2361	repressor CpxP
kpn2146_RS23680		2.1749	1.5348	1.1332	membrane protein
kpn2146_RS08600		2.1162	1.3974	1.0425	membrane protein
kpn2146_RS09400		2.0276	1.4093	1.4106	recombinase RarA
kpn2146_RS22810		1.9490	2.5118	1.3509	glycine cleavage system protein H
kpn2146_RS22510		-2.5763	-1.1859	-2.3811	ferrous iron transporter B involved in uptake

## **I. DEGs Common to All Four Gold Nanoparticles**

All four gold nanoparticles tested, including the inactive pMBA-capped conjugates, caused an up-regulation of membrane porins, the MerR family of transcriptional regulators, and Copper-Exporting ATPase. The majority of regulators in the MerR family activate transcription in response to environmental stimuli such as oxidative stress, heavy metals or antibiotics.<sup>13</sup> The inactive pMBA-capped nanoparticles caused an up-regulation of this transcription regulator, and was further up-regulated in the presence of the active antimicrobial conjugates. Experiments have shown that oxidative stress and copper resistance gene clusters are induced in bacteria living in metal-contaminated environments, conceivably to promote cellular defense.<sup>14</sup> This suggests that the inactive gold core alone may cause *K. pneumoniae* to induce a cellular protection response, even though the pMBA-capped gold nanoparticles have no inhibitory effects on the growth of the bacteria.<sup>15</sup>

## **II. DEGs Common to All Three Active Conjugates**

All three of the active conjugates induced an up-regulation of various porins, transcriptional regulators, stress response proteins, and transporters. Many transporters dedicated to the export of metals were up-regulated including a zinc/cadmium/mercury/lead-exporting ATPase, a zinc ABC transporter substrate-binding protein and an iron ABC transporter substrate-binding protein. One of the most down-regulated proteins was ferrous iron transporter B, involved in uptake of iron. The differential expression of these transport systems indicated that the bacteria were attempting to remove the heavy metals, which could include the gold nanoparticles.

A large number of proteins, lipoproteins, and enzymes related to the cell

membrane were among the most up-regulated genes. Select genes include kpn2146\_RS11060, a protein involved in cell envelope biosynthesis, and kpn2146\_RS09395, which encodes for lolA, and interacts with lolB to transfer lipoproteins from the cytosolic membrane to the outer membrane.<sup>16</sup> The up-regulation of these genes may indicate that the nanoparticles caused an alteration in the cell membrane. In addition, kpn2146\_RS25545, encoding for glycerol-3-phosphate dehydrogenase and kpn2146\_RS26690, encoding for glycerol uptake facilitator GlpF were up-regulated. These genes may be involved in phospholipid and other cellular component biosynthesis. Glycerol and glycerol-3-phosphate are precursors for phospholipid biosynthesis, as well as other essential cellular components, such as the cell wall.<sup>17</sup> Glycerol-3-phosphate dehydrogenase is an essential membrane enzyme, functioning at the central junction of respiration, glycolysis, and phospholipid biosynthesis.<sup>17</sup> The up-regulation of these genes, combined with previous knowledge that the three gold nanoparticle conjugates inhibit bacterial growth, indicated that the gold nanoparticle conjugates may be affecting cellular component biosynthesis required for cell division or proliferation. This evidence also indicated that the conjugates might significantly affect integrity of the cell membrane.

A number of genes related to the envelope stress response pathway were up-regulated. The disruption of normal protein trafficking in the cell envelope activates the Cpx Pathway.<sup>18</sup> This activation stimulates the expression of a number of genes whose products function to fold or degrade the delocalized proteins. All three active conjugates caused an up-regulation of kpn2146\_RS17190, encoding for the heat shock protein HtpX. HtpX is a zinc metalloprotease that collaborates with FtsH to degrade abnormal membrane proteins.<sup>18</sup> HtpX is under control of the Cpx Envelope Stress Response.

kpn2146-RS04105, a periplasmic protein induced by the cell envelope response pathway, was also up-regulated by all three active conjugates. However, all three active conjugates up-regulated kpn2146\_RS00385, which produced Repressor CpxP. Repressor CpxP is a small protein that blocks a regulon controlling the Cpx two component system.<sup>19</sup> Overexpression of the repressor can block activation of the pathway.<sup>19</sup> The Cpx two component regulatory system plays an important role in protection from stresses, and the repression of the pathway can lead to reduced cell survival.<sup>19</sup>

The gene expression experiments indicated that all three conjugates may be up-regulating various transporters in an attempt to remove heavy metals. All three active conjugates may also be repressing the Cpx cell envelope response. A large proportion of the most up-regulated genes were implicated in cell membrane pathways; however, further experimentation is required to determine exactly how the bacterial membrane is affected by the gold nanoparticle conjugates.

### **III. DEGs Unique to LAL-32 j**

The genes listed in Table 2.7 were the genes most up-regulated and common to all of the nanoparticle conjugates. They were analyzed to determine how the nanoparticles generally affected the bacteria. It was also of interest to determine which genes were differentially expressed only upon exposure to LAL-32 j and not by other conjugates. LAL-32 j was found to inhibit more bacterial growth than the original LAL-32 compound, and became bactericidal at 1.25  $\mu$ M. LAL-32 j also doubled the time of resistance over the original formulation. LAL-32 affected 151 genes when incubated with *K. pneumonia*, whereas LAL-32 j altered the expression of 299 genes. The approximate

doubling in gene expression was attributed to altering the feed ratio of ligand 6, as this was the only difference between the two compounds. Figure 2.6 compares the genes differentially expressed by each nanoparticle conjugate.

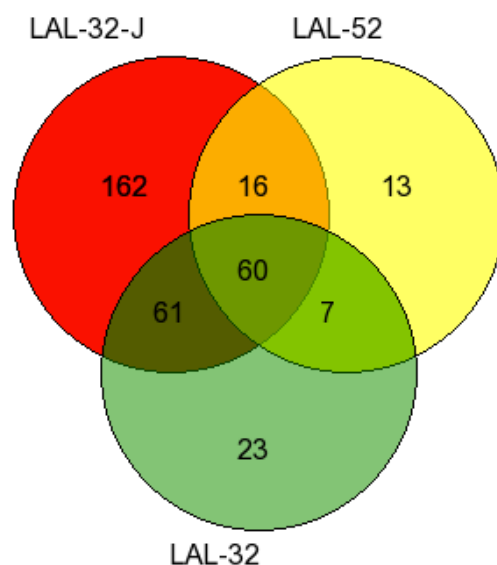


**Figure 2.6: A venn diagram comparing the genes differentially expressed upon exposure to each of the nanoparticle conjugates versus the bacteria-only control.**

Figure 2.6 illustrates 162 genes unique to conjugate LAL-32 j. Due to the large number of unique genes, only certain processes were selected for detailed analysis. It was of interest to determine how LAL-32 j more effectively inhibited the growth of the bacteria compared to LAL-32. The process gene ontology reported that LAL-32 j caused differential expression in genes related to stress response, cell division, response to antibiotics, and the cell cycle, many of which were not differentially expressed upon exposure to LAL-32. A set of unique genes was selected from these processes to further understand how the LAL-32 j conjugate increased the efficacy of bacterial growth inhibition.

**Table 2.8: The Identification, Amount of Differentiated Gene Expression, and the Gene Product for Genes Differentially Expressed in LAL-32 j Relating to Cell Division, the Response to Antibiotics, or Response to Stress**

\*Note: This is not a complete list of the differentially expressed genes. Genes selected for reporting were differentially expressed upon exposure to LAL-32 j, but not differentially expressed upon exposure to LAL-32. The genes reported are implicated in processes concerning cell division, the cell cycle, response to stress, and response to antibiotic. An absolute value of  $\text{Log}_2(\text{Treatment/Control}) \geq 1$  was used to determine statistical significance. The color scale aids in the identification of Up-Regulated (Red) and Down-Regulated (Green) genes.

Gene ID	Log <sub>2</sub> Ratio (LAL-32 j/ Bacteria-Only)	Gene Product
kpn2146_RS04340	1.4050	cell division protein MraZ
kpn2146_RS22840	1.7213	Z-ring-associated protein
kpn2146_RS19485	1.3161	cell division protein ZipA
kpn2146_RS21680	1.1885	cell division protein FtsB
kpn2146_RS09390	1.1599	cell division protein FtsK
kpn2146_RS02925	-1.1833	integrase
kpn2146_RS23455	-1.0188	transposase
kpn2146_RS23140	-1.0359	integrase
kpn2146_RS02930	-1.1948	integrase
kpn2146_RS25830	1.9419	UDP phosphate 4-deoxy-4-formamido-L-arabinose transferase
kpn2146_RS15400	1.8503	beta-lactamase
kpn2146_RS13160	1.4617	beta-lactamase
kpn2146_RS25835	1.5363	UDP-4-amino-4-deoxy-L-arabinose-oxoglutarate aminotransferase
kpn2146_RS20935	1.3404	putative multidrug efflux system membrane fusion component OqxA
kpn2146_RS25825	1.1599	bifunctional UDP-glucuronic acid decarboxylase/UDP-4-amino-4-deoxy-L-arabinose formyltransferase
kpn2146_RS09340	1.4609	cold-shock protein – inhibits DNA replication
kpn2146_RS09680	1.1094	ribosome modulation factor
kpn2146_RS07755	1.4195	universal stress protein G – associates with GroEL
kpn2146_RS11520	1.1709	dihydropteroate synthase
kpn2146_RS11115	1.0253	hydroperoxidase II
kpn2146_RS14455	1.0154	peroxiredoxin
kpn2146_RS02080	-1.0422	colicin V secretion protein CvaA
kpn2146_RS01605	-1.0812	anti-adaptor protein iraM – Stabilizes RpoS

### **i. DEGs Unique to LAL-32 j Involved in Cell Division**

Various cell-division proteins were differentially expressed with LAL-32 j, but were not expressed in LAL-32. These proteins included MraZ, a Z-ring associated protein, ZipA, and FtsB. MraZ plays a role in cell-wall biosynthesis and cell division.<sup>20</sup> FtsB is implicated in the septum-localization process during cell division.<sup>21</sup> The cell division protein FtsZ is anchored to the cytoplasmic membrane by the membrane protein ZipA.<sup>22</sup> The up-regulation of these cell division proteins may indicate the bacteria attempting to overcome a block in cell division caused by the gold nanoparticles. The FtsK gene was also up-regulated, which is an essential cell division protein that localizes at the septum. It is induced by the SOS response, a reaction to DNA damage where the cell cycle is arrested.<sup>23</sup> A SOS-inducible promoter precedes the FtsK gene, and the overexpression of FtsK has been shown to block cell division.<sup>23</sup> The additional effects on the cell division proteins seen with LAL-32 j, but not the other conjugates, may be an insight into why the efficacy of inhibition was significantly increased with the altered feed ratio conjugate. Additional experimentation is required to determine exactly how the LAL-32 j conjugate affected cell division.

### **ii. DEGs Unique to LAL-32 j Involved in Oxidative Stress**

LAL-32 j also caused the up-regulation of peroxiredoxin, and hydroperoxidase II. These enzymes help protect the cell from oxidative stress induced by hydrogen peroxide. Bacteria such as *K. pneumoniae* that grow aerobically utilize molecular oxygen ( $O_2$ ) for respiration or oxidation of nutrients.<sup>24</sup> By-products of the reactions include superoxide anion radicals ( $\cdot O_2^-$ ), hydrogen peroxide ( $H_2O_2$ ), and the highly reactive hydroxyl radicals

( $\cdot\text{OH}$ ), and are generated continuously as cells grow.<sup>24</sup> The LAL-32 j compound affected 144 metabolic genes, 33 oxidation-reduction genes, and 3 genes involved in the electron transport chain. The large up-regulation in metabolism, with presumably decreased regulation, may cause a large increase in the production of reactive oxygen species. The biological targets for these highly reactive molecules are DNA, RNA, proteins and lipids.<sup>24</sup> Lipids are a major target during oxidative stress, and the free radicals can directly attack polyunsaturated fatty acids in the membrane, which initiate peroxidation in the cell.<sup>24</sup> Lipid peroxidation decreases membrane fluidity, altering membrane properties, and may disrupt membrane-bound proteins.<sup>24</sup> An amplification process is initiated in the bacteria when the polyunsaturated fatty acids are degraded to products such as aldehydes, which themselves are very reactive and can damage molecules such as proteins.<sup>24</sup> The differential gene expression data indicated that each nanoparticle conjugate may have caused a large alteration in the bacteria membrane, which may be partially explained by the production of reactive oxygen species. The unique up-regulation of the peroxiredoxin and hydroperoxidase II genes by LAL-32 j may indicate that the LAL-32 j could have induced additional forms of oxidative stress on the cell through the production of a reactive oxygen species.

### **iii. DEGs Unique to LAL-32 j Involved in Antibiotic Resistance**

LAL-32 j uniquely induced the differential expression of a significant number of antibiotic resistance genes. The nanoparticle conjugate caused the up-regulation of beta-lactamases, the enzyme that confers resistance to beta-lactam antibiotics, including carbapenems. A multidrug efflux system membrane fusion component OqxA was up-

regulated, as well as numerous UDP genes targeted for the resistance mechanism for polymyxin and cationic antimicrobial peptides. The up-regulation of these antibiotic resistant pathways indicated that the bacterial antibiotic resistance genes had been induced, while the bacteria remained susceptible to the gold nanoparticle conjugates for nine days. The bacteria did not up-regulate any of these genes when exposed to LAL-32, which possibly indicated that LAL-32 did not have the same antibiotic threat level to the bacteria, and thereby failed to initiate the resistance pathways.

LAL-32 j doubled the time to resistance over LAL-32 in *K. pneumoniae*. This increase in time to resistance may be attributed to the down regulation of integrases and transposases upon exposure to the LAL-32 j conjugate. These genes remained unaffected after incubation with LAL-32. Transposases and integrases are proteins that mediate the recombination reaction in which discrete DNA segments are transferred between nonhomologous sites.<sup>25</sup> Many antibiotic resistance genes are encoded on plasmids or transposons, and can be transferred to other bacteria.<sup>26</sup> The horizontal gene transfer of antibiotic resistance has led to wide-spread resistance as well as multi-drug resistant pathogens. The down-regulation of the integrases and transposases upon incubation with LAL-32 j indicated that the feed ratio of the thiol ligands in the monolayer might affect resistance mechanisms, as well as the dissemination of antibiotic resistant genes.

There is a possibility that the down-regulation of the integrase and transposase genes was attributed to the splicing of the cassette from the replicative chromosome in an action to transfer the genes to another bacterium. If the bacteria were up-regulating genes for widespread resistance after four hours of incubation with the gold-nanoparticles, it would imply that the bacteria do not possess the gene cassettes necessary for gold-

nanoparticle resistance. The bacteria remained susceptible to the gold-nanoparticle conjugates for nine days with sub-inhibitory concentrations of treatment.

LAL-32 j was created by taking the LAL-32 conjugate designed for *E. coli*, and decreasing the feed ratio of ligand 6. This resulting conjugate was able to overcome the extracellular polysaccharide capsule of *K. pneumoniae* and became bactericidal at 1.25  $\mu\text{M}$ . Bactericidal compounds that kill the microbes instead of inhibiting growth may aid in the avoidance of antibiotic resistance, since they decrease the number of bacteria available to undergo a spontaneous genetic mutation allowing for antibiotic resistance. LAL-32 j induced the differential expression of 299 genes in *K. pneumoniae* versus the 151 genes differentially expressed with LAL-32. The much larger increase in gene expression may indicate that the LAL-32 j more significantly affected the bacteria.

#### **LAL-32 j Tested Against *M. avium* and *M. Abscessus***

An experiment was then performed to determine if LAL-32 j was effective against *Mycobacterium avium* (MAC 104WT) and *Mycobacterium abscessus* (ATCC 19977). These bacteria are opportunistic pathogens and contain a thicker cell wall coated by a waxy, hydrophobic, mycolic acid layer.<sup>27</sup> This mycolic acid layer makes it difficult for many compounds, including antibiotics, to reach intracellular targets. The LAL-32 j compound was tested against *M. avium* and *M. abscessus* in concentrations up to 10  $\mu\text{M}$ . All samples tested were turbid upon visual analysis, and plating and colony counting found no significant levels of bacterial growth inhibition at concentrations tested.

The Feldheim Lab showed that both the identity of ligands and their feed ratios in the monolayer of the gold nanoparticle greatly affected the antimicrobial properties of the

nanoparticle.<sup>6</sup> The feed ratio of ligand 6 turned one of the *E. coli* conjugates into a conjugate highly active toward *K. pneumoniae*. This conjugate however, was ineffective against *M. avium* and *M. abscessus*. It is possible that the gold-nanoparticles are narrow-spectrum antibiotics. Narrow spectrum antibiotics are only effective against a certain bacteria, or group of bacterium, and are administered when the causative agent of the infection is known.<sup>28</sup> One benefit of narrow-spectrum antibiotics are that they cause less antibiotic resistance because they deal only with specific bacteria.<sup>28</sup> Further experimentation is required to determine which bacterial species may be affected by LAL-32 j.

## Bibliography

- [1] The Genome Institute at Washington University, Genome: *Klebsiella pneumoniae*, 2014: <http://genome.wustl.edu/genomes/detail/klebsiella-pneumoniae/>
- [2] Campos, M. A.; Vargas, M. A.; Regueiro, V.; Llompert, C. M.; Albertí, S.; Bengoechea, J. A. *Infect. Immun.* **2004**, *72*, 7107–7114.
- [3] Slack, M. P. E.; Nichols, W. W. *J. Antimicrob. Chemother.* **1982**, *10*, 368–372.
- [4] ATCC, NDM-1 Strains, **2013**  
<http://www.atcc.org/~media/F692E3D016E5434AB7C3E43EE26395E7.aspx>
- [5] ATCC, *Escherichia coli* (Migula) Castellani and Chalmers (ATCC® 25922™), **2013**.  
<https://www.atcc.org/products/all/25922.aspx?slp=1#documentation>
- [6] Bresee, J.; Bond, C. M.; Worthington, R. J.; Smith, C. A.; Gifford, J. C.; Simpson, C. A.; Carter, C. J.; Wang, G.; Hartman, J.; Osbaugh, N. A.; Shoemaker, R. K.; Melander, C.; Feldheim, D. L. *J. Am. Chem. Soc.* **2014**, *136*, 5295–5300.
- [7] Gifford, J. C.; Bresee, J.; Carter, C. J.; Wang, G.; Melander, R. J.; Melander, C.; Feldheim, D. L. *Chem. Commun.* **2014**, *50*, 15860–15863.
- [8] Pankey, G. A.; Sabath, L. D. *Clin Infect Dis.* **2004**, *38*, 864–870.
- [9] Santana, C.; Segura, D.; Sánchez, S. *Rev. Latinoam. Microbiol.* **1994**, *36*, 139–158.
- [10] Klussmann, E.; Scott, J. *Protein-Protein Interactions as New Drug Targets*; Springer Science & Business Media, **2008**.
- [11] Mitrophanov, A. Y.; Groisman, E. A. *Genes Dev* **2008**, *22*, 2601–2611.
- [12] Poole, K. *J. Antimicrob. Chemother.* **2012**, dks196.
- [13] Brown, N. L.; Stoyanov, J. V.; Kidd, S. P.; Hobman, J. L. *FEMS Microbiol. Rev.* **2003**, *27*, 145–163.
- [14] Wiesemann, N.; Mohr, J.; Grosse, C.; Herzberg, M.; Hause, G.; Reith, F.; Nies, D. *H. J. Bacteriol.* **2013**, *195*, 2298–2308.
- [15] Bresee, J.; Bond, C. M.; Worthington, R. J.; Smith, C. A.; Gifford, J. C.; Simpson, C. A.; Carter, C. J.; Wang, G.; Hartman, J.; Osbaugh, N. A.; Shoemaker, R. K.; Melander, C.; Feldheim, D. L. *J. Am. Chem. Soc.* **2014**, *136*, 5295–5300.

- [16] Yokota, N.; Kuroda, T.; Matsuyama, S.; Tokuda, H. *J. Biol. Chem.* **1999**, *274*, 30995–30999.
- [17] Yeh, J. I.; Chinte, U.; Du, S. *PNAS* **2008**, *105*, 3280–3285.
- [18] Shimohata, N.; Chiba, S.; Saikawa, N.; Ito, K.; Akiyama, Y. *Genes to Cells* **2002**, *7*, 653–662.
- [19] Raivio, T. L.; Popkin, D. L.; Silhavy, T. J. *J. Bacteriol.* **1999**, *181*, 5263–5272.
- [20] Adams, M. A.; Udell, C. M.; Pal, G. P.; Jia, Z. *Acta Crystallogr Sect F Struct Biol Cryst Commun* **2005**, *61*, 378–380.
- [21] Buddelmeijer, N.; Beckwith, J. *Mol. Microbiol.* **2004**, *52*, 1315–1327.
- [22] Pazos, M.; Natale, P.; Vicente, M. *J. Biol. Chem.* **2013**, *288*, 3219–3226.
- [23] Draper, G. C.; McLennan, N.; Begg, K.; Masters, M.; Donachie, W. D. *J. Bacteriol.* **1998**, *180*, 4621–4627.
- [24] Cabiscol, E.; Tamarit, J.; Ros, J. *Int. Microbiol.* **2000**, *3*, 3–8.
- [25] Craig, N. L. In *eLS*; John Wiley & Sons, Ltd, **2001**.
- [26] Barlow, M. *Methods Mol. Biol.* **2009**, *532*, 397–411.
- [27] Brennan, P. J. *Tuberculosis (Edinb)* **2003**, *83*, 91–97.
- [28] Narrow Spectrum Antibiotics, SRS Pharmaceuticals, <http://www.srspharma.com/narrow-spectrum-antibiotics.htm>

### III. Conclusion

The nanoparticle conjugates previously designed for *E. coli* were effective inhibitors against *K. pneumoniae*. LAL-32 and LAL-52 had the lowest MIC<sub>99,9</sub> of 0.625  $\mu$ M and were therefore chosen for further testing. LAL-32 had feed ratios of 33x, 46x, and 33x for ligands 5, 6 and 8 respectively. Altering the feed ratio of ligand 6 to 33x produced conjugate LAL-32 j, which became bactericidal at 1.25  $\mu$ M. LAL-32 j was also able to double the time to resistance over the original LAL-32 conjugate. *K. pneumoniae* took twelve days to become resistant to LAL-52, which had feed ratios of 33x, 46x, and 16.5x for ligands 5, 6 and 11 respectively. These experiments indicated that the ratio and identity of the thiol ligands in the monolayer greatly affect the antimicrobial efficacy and the time to resistance for the nanoparticles. The resistance assay also indicated that bacteria that are continually exposed to the inactive pMBA-capped nanoparticles remain sensitive to the active conjugates. Bacteria that were resistant to one conjugate were also resistant to all variants tested, indicating a similar mode of action for LAL-52 and LAL-32, as well as the altered feed-ratio variants.

The differential gene expression experiment demonstrated that LAL-32 j significantly affected a greater number of genes than the original conjugate LAL-32. Gold nanoparticles with greater antimicrobial efficacy may affect the bacteria more than the less active conjugates. The gene expression assay also indicated that the pMBA-capped nanoparticles affected the expression of only eighteen genes in the *K. pneumoniae*. The pMBA-capped nanoparticles up-regulated genes implicated with environmental heavy metals, but had no effect on the growth of the bacteria. This increase in gene expression implied that the mixed-ligand monolayer conjugates

primarily inhibit the growth of the bacteria, and the sole presence of the gold core did not considerably affect the bacteria.

Each of the three active conjugates tested greatly altered the expression of bacterial metabolism, and the genes implicated in the structure of the cell membrane in slightly different ways. Additional experimentation is required to determine how the nanoparticles are affecting the bacteria. The conjugate with the most antimicrobial efficacy, LAL-32 j, also affected a number of cell division and antibiotic resistance pathways. The antibiotic resistance pathways were induced in the bacteria after four hours of incubation with LAL-32 j, but the bacteria remained sensitive to the conjugate for nine days. This experiment implied that the innate antibiotic resistance genes present in the *K. pneumoniae* strain were not able to overcome the gold nanoparticles.

The gold nanoparticle conjugate LAL-32 j was found to be ineffective against *M. avium* and *M. abscessus*. This may indicate that the gold nanoparticles are narrow spectrum antibiotics; however, further experimentation is required to determine which bacteria are sensitive to the LAL-32 j conjugate. LAL-32 j demonstrated the possibility for the gold nanoparticles to delay the onset of antibiotic resistance. LAL-32 j doubled the time to resistance over the original LAL-32 compound, and is bactericidal at 1.25  $\mu\text{M}$ . Bactericidal compounds decrease the overall number of cells, and therefore the probability of a spontaneous genetic mutation to confer antibiotic resistance. If LAL-32 j is specific toward certain bacterial groups, it may aid in the problem of multi-drug resistant pathogens. Bacteria unaffected by the gold nanoparticles would not likely gain nor pass on resistant genes. These experiments demonstrated that the identity and ratio of ligands in the monolayer of the gold nanoparticle affect the antimicrobial efficacy of the

conjugate as well as the time to resistance. The active gold nanoparticle conjugates may be further improved by altering the ligands in the monolayer to further avoid the serious problem of antibiotic resistance.